

UC Berkeley
SEMM Reports Series

Title

A Simple and Efficient Finite Element for General Shell Analysis

Permalink

<https://escholarship.org/uc/item/63n1w6nq>

Author

Kanok-Nukulchai, Worsak

Publication Date

1978

NISEE/COMPUTER APPLICATIONS
DAVIS HALL
UNIVERSITY OF CALIFORNIA
BERKELEY, CALIFORNIA 94720
(415) 642-5113

Report no.
UC SESM 78-1

STRUCTURAL ENGINEERING AND STRUCTURAL MECHANICS

**A SIMPLE AND EFFICIENT FINITE ELEMENT
FOR GENERAL SHELL ANALYSIS**

by

WORSAK KANOKNUKULCHAI

JANUARY 1978

DEPARTMENT OF CIVIL ENGINEERING
UNIVERSITY OF CALIFORNIA
BERKELEY, CALIFORNIA

Division of Structural Engineering and Structural Mechanics
Department of Civil Engineering, University of California
Berkeley, California.

Report No. 78-1

**A SIMPLE AND EFFICIENT FINITE ELEMENT FOR
GENERAL SHELL ANALYSIS**

by

WORSAK KANOK-NUKULCHAI

Graduate student and research assistant

This report was prepared under contract number

DOT - HS - 6 - 01443

Faculty Investigators

J.L. SACKMAN

R.L. TAYLOR

sponsored by

National Highway Traffic Safety Administration
Department of Transportation
Washington, D.C.

January 1978

TABLE OF CONTENTS

	<u>Page</u>
ACKNOWLEDGEMENTS.....	iii
ABSTRACT.....	iv
INTRODUCTION.....	1
SHELL ELEMENT STRATEGIES.....	1
3-D Continuum Elements.....	1
Classical Shell Elements.....	2
Degenerated Shell Elements.....	2
THE BILINEAR DEGENERATED SHELL (BDS) ELEMENT.....	3
Geometry and Displacement Field.....	3
Stresses - Strains.....	5
Derivation of Element Stiffness.....	6
Torsional Effect.....	8
NUMERICAL EXAMPLES.....	10
Thin Cylindrical Shell Roof.....	10
Clamped Hyperbolic Paraboloid Shell.....	10
Thick Cylindrical Shell.....	10
Arch Dam.....	10
Curved Box Girder.....	10
CONCLUSIONS.....	11
REFERENCES.....	12
FIGURES.....	14
APPENDIX A: Shell Stress-Resultants.....	34
B: Element Manual.....	35
C: Listing of the Element Subroutines.....	37

ACKNOWLEDGEMENTS

This report was prepared under the contract no. DOT-HS-6-01443; sponsored by the National Highway Traffic Safety Administration of the Department of Transportation, administered by Dr. L. Ovenshire. The project is under the supervision of Professors R.L. Taylor and J.L. Sackman of the Department of Civil Engineering, University of California at Berkeley, and Professor T.J.R. Hughes of the Division of Engineering and Applied Science, California Institute of Technology, Pasadena, California.

Acknowledgement is also extended to his colleagues, A. Curnier, J. Rollins and Dr. H. Hilber for their continued interest.

A SIMPLE AND EFFICIENT FINITE ELEMENT FOR GENERAL SHELL ANALYSIS.

WORSAK KANOK-NUKULCHAI

Division of Structural Engineering and Structural Mechanics,
Department of Civil Engineering, University of California
Berkeley, California, U.S.A.

ABSTRACT

A simple, efficient and versatile finite element is introduced for shell applications. The element is developed based on a degeneration concept, in which the displacements and rotations of the shell mid-surface are independent variables. Bilinear functions are employed in conjunction with a reduced integration for the transverse shear energy. Several examples are tested to demonstrate the effectiveness and versatility of the element. The numerical results indicate that the shell element performs accurately for both thick and thin shell situations.

A SIMPLE AND EFFICIENT FINITE ELEMENT FOR GENERAL SHELL ANALYSIS.

WORSAK KANOK-NUKULCHAI

Division of Structural Engineering and Structural Mechanics,
Department of Civil Engineering, University of California
Berkeley, California, U.S.A.

INTRODUCTION

The importance of shell structures and their generic analysis complexities has naturally lead to a reliance on the finite element method for the solution to many types of shell problems. This, of course, requires a finite element representation of the shell behavior and over the last 20 years many elements have been developed and employed in a multitude of programs. A history of shell elements is traced in [1,2] and only a brief summary will be included here. The paper's main theme is the development of a new shell element: the (B)ilinear (D)egenerated (S)hell. The BDS element attempts to rectify problems inherent to most shell elements: (a) the limited scope of problems which can be solved and, (b) the high formulation cost of computing the element stiffness. The former restricts most elements to one class of shells, either thin or thick shells, depending on the parent theory used for developing the element. The element stiffness formulation may not be a cost factor for most linear problems but is of paramount importance in nonlinear formulations. Thus the quest for the ideal shell element that is universally applicable and cheap to use was a motivating force in the present study.

The approach taken in this paper explores an avenue that was successfully exploited by Hughes et.al. [3] for developing a simple bilinear plate element. The element in [3] was based on a one-point quadrature for the transverse shear strain energy. The solution, despite its simplicity, is surprisingly accurate for both thick and thin plates.

SHELL ELEMENT STRATEGIES

A shell element can be classified as a 3-D continuum, a classical shell, or a degenerated shell. Figure 1 portrays a skeletal outline of these classifications. To complement Figure 1, a brief paragraph will describe the highlights as they relate to the main theme of this paper. The details of previous shell formulations are contained in the references and the reader is referred to them for a detailed understanding of the development of previous shell elements.

3-D Continuum Elements

The three dimensional field equations can be processed to form a 3-D continuum

* Graduate student and research assistant

element, Figure 1. This, of course, produces an element that is ignorant of the usual kinematic constraints, or assumptions, of most shell problems. Popular among these is: the thickness of the shell is small compared to the other dimensions. Coupled to this is that the shell generally carries load via bending and membrane action. The 3-D formulation is now at a distinct disadvantage: several layers of elements or higher order elements are required to portray bending. Thus economic considerations usually curtail the usefulness of this element. In addition, a 3-D element is found to fail at a moderate length to thickness aspect ratio due to displacement locking through the thickness. Wilson [4] suggested the use of incompatible displacement modes to improve the basic 3-D thick shell performance. Dovey [2] followed with a study of both the reduced integration technique and the idea of adding incompatible modes. These modifications do produce the desired effect, a more flexible shell behavior hence better performance. However, the convergence of these modified 3-D elements can not be guaranteed [2].

Classical Shell Elements

The classical shell element is derived by reducing the 3-D field equations to a particular class of shell equations using analytical integration over the thickness while employing shell assumptions. Common assumptions take advantage of one or more facets of the shell geometry such as the rotation of the cross-section is simply the slope of the shell. This applies only when the shell is relatively thin and its shear strain is negligible. As a result the normal to the reference surface remains normal. This is the *Kirchhoff-Love hypothesis*. Since most shell elements of classical type invoke this assumption, its implications will be reviewed. The Kirchhoff-Love hypothesis leads to displacement equations of equilibrium that are a coupled set of two second-order differential equations inplane and a fourth-order differential equation in the transverse direction of the shell. Therefore, a shell element based on this theory needs C^1 continuity, thus, higher order interpolation functions are required than for the 3-D continuum. Nodal variables must include at least three displacements and two derivatives of the transverse displacement. The inplane, membrane, interpolation functions are usually of lower order than the transverse, bending, function. This can create gaps or overlaps between the edges of two non-planar elements. Many shell elements and shell theories also lack the presence of rigid body modes. Despite these shortcomings many elements are reported to work satisfactorily in the linear infinitesimal-displacement regime [4,5,6].

Degenerated Shell Elements

The degeneration concept described in Figure 1 directly discretizes the 3-D field equation in terms of mid-surface nodal variables. This usually employs a shell assumption, i.e., *the straight normal at any point on the mid-surface remains straight*. The formulation also includes the transverse shear effect, thus no Kirchhoff-Love hypothesis is presumed. The equilibrium equations in terms of independent variables (e.g., displacements and rotations) are second-order differential equations, therefore, the elements require only C^0 -continuous shape functions.

Many authors [7,8,9,10] who developed shell elements based on this concept obtained unsatisfactory results when these elements are applied in the thin shell regime. The difficulty can be traced to the transverse shear energy which is $O[(L/h)^2]$ higher than the remaining terms, where L/h denotes the element length to thickness aspect ratio. Thus as the thickness approaches zero, the computed shear stiffness completely dominates, and no effect of the bending stiffness remains with a finite computer word length. As a result, the element produces an excessively stiff solution which does not reflect the correct bending behavior. Physically, this phenomenon is known as a *shear-locking* [3].

Several techniques have been studied in an attempt to solve the shear-locking problem. Wempner [10] introduced a *discrete Kirchhoff hypothesis* which enforced the Kirchhoff hypothesis only at the mid-side of the elements. The poor performance of this element was

due, presumably, to too many constraints being enforced. The correction employed in [10] was to reduce the number of constraints. All shear energy was suppressed and good results were obtained. The element with no shear energy reverts to being good for only thin shells hence this solution is wanting. In addition the technique used in [10] leads to either unsymmetric coefficient matrices to be solved for the nodal displacements or an increased number of unknowns if Lagrange multiplier methods are used to satisfy the constraints. Zienkiewicz et.al. [11] retained the transverse shear energy but used reduced integration for quadratic and cubic isoparametric serendipity elements [12] and obtained good results for some thin and thick shells. In this formulation, the transverse shear strain energy in the thin shell situation is a penalty function for the Kirchhoff-Love hypothesis and requires under integration to avoid the locking effect [13]. For certain boundary conditions, however, this element shows a tendency to lock in thin shell analysis due to the additional constraints imposed by the boundary conditions.

THE BILINEAR DEGENERATED SHELL ELEMENT

The BDS element (Figure 2) evolves from an eight-node three dimensional brick. The mid-surface, enclosed by four straight sides, forms a hyperbolic paraboloid and, as the name implies, the concept of degeneration is used. Due to the simplicity of the bilinear mid-surface geometry and the displacement field, the strain energy can be integrated analytically over the shell thickness. The integration over the reference mid-surface can then be performed numerically. This not only simplifies the derivation but also saves computer effort in formulating the element stiffness. The rigid body modes are present since this is an isoparametric element. The transverse shear strain energy is retained, consequently, the element is applicable to either thick or thin shells. Only one-point numerical integration is used for this shear strain energy at the center of the element to avoid the shear-locking effect. The element, when applied to plates is equivalent to the plate element presented in [3].

Several examples are tested using the BDS element. The results show that the element is capable of performing accurately for both thin and thick shells. The details of the formulation are now presented.

Geometry and Displacement Field

The shell element, Figure 2, is defined by the natural, curvilinear coordinates, $\{r,s,t\}$ such that a bi-unit cube is uniquely mapped into the shell element. As the thickness of the shell element is being input in the direction normal to the mid-surface at each node, the position at any point in the element can be uniquely given in terms of nodal coordinates and thicknesses as

$$\mathbf{x}(r,s,t) = \sum_{I=1}^4 N^I(r,s) \left\{ \mathbf{x}^I + \frac{1}{2} t h^I \hat{\mathbf{e}}_{z_3}^I \right\} \quad (1)$$

where \mathbf{x}^I are the coordinates of the mid-surface, h^I the thickness and $\hat{\mathbf{e}}_{z_3}^I$ the normal unit vector, all at a node I. The interpolation function N^I is bilinear, i.e.,

$$N^I(r,s) = \frac{1}{4} (1+r^I r) (1+s^I s) \quad (2)$$

where r^I, s^I are the natural coordinates of node I.

At any point on the mid-surface, an orthogonal set of local coordinates, $\{ \mathbf{z} \}$, is constructed such that its unit vectors are:

$$\hat{\mathbf{e}}_{z_3}(r,s) = \mathbf{x}_{,r}(r,s) \times \mathbf{x}_{,s}(r,s) / |\mathbf{x}_{,r} \times \mathbf{x}_{,s}| \quad (3)$$

$$\hat{\mathbf{e}}_{z_2}(r,s) = \hat{\mathbf{e}}_{z_3}(r,s) \times \mathbf{x}_{,r}(0,0) / |\hat{\mathbf{e}}_{z_3} \times \mathbf{x}_{,r}(0,0)| \quad (4)$$

$$\hat{\mathbf{e}}_{z_1}(r,s) = \hat{\mathbf{e}}_{z_2}(r,s) \times \hat{\mathbf{e}}_{z_3}(r,s) \quad (5)$$

The first is normal, while the others are tangent to the midsurface at a point $(r,s,0)$ on the mid-surface (Figure 2).

The displacement vector at any point (r,s,t) in the element can be given in the form:

$$\mathbf{u}(r,s,t) = \sum_l N^l(r,s) \{ \mathbf{u}^l + \mathbf{u}_\alpha^l(t) \} \quad (6)$$

where \mathbf{u}^l is the nodal displacement vector on the mid-surface, and \mathbf{u}_α^l is the relative nodal displacement vector produced by a normal rotation at the node. The vector \mathbf{u}_α^l is to be expressed explicitly in terms of the rotation vector, $\boldsymbol{\alpha}^l$, about each of the global axes at the node. Using the shell assumption that *straight normals to the reference mid-surface remain straight after deformation*, the displacement vector based on the local \mathbf{z} coordinates, produced by the normal rotation $\boldsymbol{\alpha}^l$ about local axes, is \mathbf{w}_α and expressed by

$$\mathbf{w}_\alpha(t) = \frac{1}{2} t h \begin{Bmatrix} \alpha_2^l \\ -\alpha_1^l \\ 0 \end{Bmatrix} \quad (7)$$

For infinitesimal rotations, the usual transformations from \mathbf{w}_α^l to \mathbf{u}_α^l and $\boldsymbol{\alpha}^{l'}$ to $\boldsymbol{\alpha}^l$, in view of (7) lead to

$$\mathbf{u}_\alpha^l(t) = \frac{1}{2} t h^l \boldsymbol{\Phi}^l \boldsymbol{\alpha}^l \quad (8)$$

where

$$\boldsymbol{\Phi}^l = \begin{bmatrix} 0 & \theta_{33}^l & -\theta_{23}^l \\ -\theta_{33}^l & 0 & \theta_{13}^l \\ \theta_{23}^l & -\theta_{13}^l & 0 \end{bmatrix} \quad (9)$$

in which θ_{ij} denotes the direction cosine from global to local coordinates, i.e.,

$$\theta_{ij} = (\hat{\mathbf{e}}_{x_i}, \hat{\mathbf{e}}_{z_j}) \quad (10)$$

Substituting (8) into (6) yields the expression of the displacement vector at any point in the shell element in terms of nodal variables:

$$\mathbf{u}(r,s,t) = \sum_i N^i(r,s) \left\{ \mathbf{u}' + \frac{1}{2} t h^i \Phi^i \alpha^i \right\} \quad (11)$$

Stresses - Strains

At any point in the shell element, the local strain components of interest are

$$\boldsymbol{\epsilon}(r,s,t) \equiv \begin{Bmatrix} \epsilon_{11} \\ \epsilon_{22} \\ \epsilon_{12} \\ \epsilon_{13} \\ \epsilon_{23} \end{Bmatrix} = \begin{Bmatrix} w_1/z_1 \\ w_2/z_2 \\ w_1/z_2 + w_2/z_1 \\ w_1/z_3 + w_3/z_1 \\ w_2/z_3 + w_3/z_2 \end{Bmatrix} \quad (12)$$

The symbol $(\cdot)/z_i$ defines a derivative with respect to local curvilinear coordinates. The derivation of these strain components can be achieved by using the second-order tensor transformation of the displacement gradients, i.e.,

$$\begin{bmatrix} w_1/z_1 & w_2/z_1 & w_3/z_1 \\ w_1/z_2 & w_2/z_2 & w_3/z_2 \\ w_1/z_3 & w_2/z_3 & w_3/z_3 \end{bmatrix} = \Theta^T \begin{bmatrix} u_{1,x_1} & u_{2,x_1} & u_{3,x_1} \\ u_{1,x_2} & u_{2,x_2} & u_{3,x_2} \\ u_{1,x_3} & u_{2,x_3} & u_{3,x_3} \end{bmatrix} \Theta \quad (13)$$

where $(\cdot)_{,x_i}$ denotes a partial derivative with respect to the global cartesian coordinates and $\Theta \equiv [\theta_{ij}]$ is the transformation matrix defined in (10).

For a linear isotropic elastic material, the local stress components are obtained from the usual shell constitutive equations which assume a state of plane stress in each lamina. Accordingly

$$\boldsymbol{\sigma}(r,s,t) = \mathbf{D} \boldsymbol{\epsilon}(r,s,t) \quad (14)$$

where $\boldsymbol{\sigma}(r,s,t) \equiv [\sigma_{11} \ \sigma_{22} \ \sigma_{12} \ \sigma_{13} \ \sigma_{23}]^T$ is the local stress vector and

$$\mathbf{D} = \begin{bmatrix} \bar{\lambda} + 2\mu & \bar{\lambda} & 0 & 0 & 0 \\ \bar{\lambda} & \bar{\lambda} + 2\mu & 0 & 0 & 0 \\ 0 & 0 & \mu & 0 & 0 \\ 0 & 0 & 0 & \mu/\kappa_s & 0 \\ 0 & 0 & 0 & 0 & \mu/\kappa_s \end{bmatrix} \quad (15)$$

in which κ_s is a shear deformation correction (1.2 is used for BDS), μ is the shear modulus, and $\bar{\lambda}$ is the plane-stress reduced Lamé constant, i.e., $\bar{\lambda} = \nu E / (1 - \nu^2)$, where E is the modulus

of elasticity and ν is Poisson ratio.

Derivation of the Element Stiffness

The standard form of the element stiffness, as derived by the general finite element procedure, is [20]

$$\mathbf{K}^{IJ} = \int_V (\mathbf{B}^I)^T \mathbf{D} \mathbf{B}^J dV \quad (16)$$

in which \mathbf{B}^I is the standard strain matrix relating the local strain vector to the nodal variables $\delta^I \equiv [\mathbf{u}^I, \alpha^I]^T$ such that

$$\epsilon(r,s,t) = \sum_I \mathbf{B}^I \delta^I \quad (17)$$

It is convenient to split the stiffness in (16) into two parts : the transverse shear effect and the bending and membrane effects. This will allow use of an appropriate order of numerical integration for each part. Accordingly, let

$$\mathbf{K}^{IJ} = \mathbf{K}_m^{IJ} + \mathbf{K}_s^{IJ} \quad (18)$$

where

$$\mathbf{K}_m^{IJ} = \int_V (\mathbf{B}_m^I)^T \mathbf{D}_m \mathbf{B}_m^J dV \quad (19)$$

$$\mathbf{K}_s^{IJ} = \int_V (\mathbf{B}_s^I)^T \mathbf{D}_s \mathbf{B}_s^J dV \quad (20)$$

and \mathbf{B}_m , \mathbf{B}_s , \mathbf{D}_m , \mathbf{D}_s are defined according to

$$\epsilon_m \equiv [\epsilon_{11} \ \epsilon_{22} \ \epsilon_{12}]^T = \sum_I \mathbf{B}_m^I \delta^I \quad (21)$$

$$\epsilon_s \equiv [\epsilon_{13} \ \epsilon_{23}]^T = \sum_I \mathbf{B}_s^I \delta^I \quad (22)$$

$$\mathbf{D} = \begin{bmatrix} \mathbf{D}_m & \underline{0} \\ \underline{0} & \mathbf{D}_s \end{bmatrix} \quad (23)$$

To formulate the matrices \mathbf{B}_m and \mathbf{B}_s , substitute (11) into (13) and the result into (12) to yield

$$\begin{Bmatrix} \epsilon_m(r,s,t) \\ \epsilon_s(r,s,t) \end{Bmatrix} = \sum_I \begin{bmatrix} \mathbf{B}_{1m}^I & \mathbf{B}_{2m}^I + t \mathbf{B}_{3m}^I \\ \mathbf{B}_{1s}^I & \mathbf{B}_{2s}^I + t \mathbf{B}_{3s}^I \end{bmatrix} \begin{Bmatrix} \mathbf{u}^I \\ \alpha^I \end{Bmatrix} \quad (24)$$

in which

$$\mathbf{B}'_m = \mathbf{L}_m(N^I) \Theta^T \quad (25a)$$

$$\mathbf{B}'_s = \mathbf{L}_s(N^I) \Theta^T \quad (25b)$$

$$\mathbf{B}'_{2m} = \frac{1}{2} h^I N^I \mathbf{L}_m(t) \Theta^T \Phi^I \quad (25c)$$

$$\mathbf{B}'_{2s} = \frac{1}{2} h^I N^I \mathbf{L}_s(t) \Theta^T \Phi^I \quad (25d)$$

$$\mathbf{B}'_{3m} = \frac{1}{2} h^I \mathbf{L}_m(N^I) \Theta^T \Phi^I \quad (25e)$$

$$\mathbf{B}'_{3s} = \frac{1}{2} h^I \mathbf{L}_s(N^I) \Theta^T \Phi^I \quad (25f)$$

The operators $\mathbf{L}_m(\cdot)$ and $\mathbf{L}_s(\cdot)$ are gradient operators with respect to local coordinates which are defined as

$$\mathbf{L}_m(f) = \begin{bmatrix} \sum_k \theta_{k1} f_{,x_k} & 0 & 0 \\ 0 & \sum_k \theta_{k2} f_{,x_k} & 0 \\ \sum_k \theta_{k2} f_{,x_k} & \sum_k \theta_{k1} f_{,x_k} & 0 \end{bmatrix} \quad (26)$$

and

$$\mathbf{L}_s(f) = \begin{bmatrix} \sum_k \theta_{k3} f_{,x_k} & 0 & \sum_k \theta_{k1} f_{,x_k} \\ 0 & \sum_k \theta_{k3} f_{,x_k} & \sum_k \theta_{k2} f_{,x_k} \end{bmatrix} \quad (27)$$

Physically, \mathbf{B}'_I is the strain contribution of the inplane displacements at node I, and $\mathbf{B}'_2 + t\mathbf{B}'_3$ is the strain contribution of the rotations at node I, which also includes the curvature effect.

Taking into account the way the local coordinates $\{\mathbf{z}\}$ are constructed, it can be shown via an orthogonality condition that

$$\mathbf{L}_m(t) = \underline{\underline{0}} \quad (28)$$

which results in

$$\mathbf{B}'_{2m} = \underline{\underline{0}} \quad (29)$$

Substituting (24) into (19), in view of (21) and (29), results in

$$\mathbf{K}_m^{IJ} = \int_{-1}^1 \int_{-1}^1 \int_{-1}^1 \begin{bmatrix} (\mathbf{B}_{1m}^I)^T \mathbf{D}_m \mathbf{B}_{1m}^J & t(\mathbf{B}_{3m}^I)^T \mathbf{D}_m \mathbf{B}_{1m}^J \\ t(\mathbf{B}_{1m}^I)^T \mathbf{D}_m \mathbf{B}_{3m}^J & t^2(\mathbf{B}_{3m}^I)^T \mathbf{D}_m \mathbf{B}_{3m}^J \end{bmatrix} |J(r,s,t)| dr ds dt \quad (30)$$

where $|J|$ is the determinant of the Jacobian matrix obtained from (1). To be consistent with the shell assumption of straight normals, $|J(r,s,t)|$ can be approximated by $|J(r,s,0)|$. Since \mathbf{B}_1 and \mathbf{B}_3 are functions of r and s only, the integral in (30) can be analytically integrated with respect to t which leads to

$$\mathbf{K}_m^{IJ} = \int_{-1}^1 \int_{-1}^1 \begin{bmatrix} 2(\mathbf{B}_{1m}^I)^T \mathbf{D}_m \mathbf{B}_{1m}^J & 0 \\ 0 & \frac{2}{3}(\mathbf{B}_{3m}^I)^T \mathbf{D}_m \mathbf{B}_{3m}^J \end{bmatrix} |J(r,s,0)| dr ds \quad (31)$$

Similarly, the shear part in (20) can be obtained as

$$\mathbf{K}_s^{IJ} = \int_{-1}^1 \int_{-1}^1 \begin{bmatrix} 2(\mathbf{B}_{1s}^I)^T \mathbf{D}_s \mathbf{B}_{1s}^J & 2(\mathbf{B}_{1s}^I)^T \mathbf{D}_s \mathbf{B}_{2s}^J \\ 2(\mathbf{B}_{2s}^I)^T \mathbf{D}_s \mathbf{B}_{1s}^J & 2(\mathbf{B}_{2s}^I)^T \mathbf{D}_s \mathbf{B}_{2s}^J + \frac{2}{3}(\mathbf{B}_{3s}^I)^T \mathbf{D}_s \mathbf{B}_{3s}^J \end{bmatrix} |J(r,s,0)| dr ds \quad (32)$$

The numerical integration is then used to evaluate the remaining integrals in (31) and (32). A two-by-two Gaussian quadrature is employed for the integral in (31) and, as mentioned before, a one-point Gaussian quadrature for the integral in (32). This will ensure singularity of the \mathbf{K}_s^{IJ} which is necessary in order to avoid the shear-locking phenomenon.

Torsional Effect

In using a bilinear-element assemblage to approximate curved shells, convergence is spoiled by a weakly-restrained torsional mode after the mesh reaches some state of refinement. The reason can be explained as follows: The BDS element employs six degrees of freedom per node, however, no stiffness corresponding to the torsional-rotation degree of freedom exists locally in the formulation. All the resistance to this rotation at each node I comes directly from the coupling of the α -rotations of the non-planar elements surrounding node I . When the finite-element mesh is refined, angles of the kinks between these elements are close to 2π and the coupling effect is reduced. This weak coupling only generates a minute amount of stiffness for the torsional rotation. Therefore, any slight disturbance in the generalized load corresponding to this degree of freedom can amplify the torsional mode to an unrealistic amount, which affects the global solution.

This problem is common to many shell elements which use six global degrees of freedom per node. In the past, a fictitious torsional spring was added either locally at the element level, or in some pseudo-normal direction defined at each node. This technique often is found unsatisfactory, especially for a flexible system in which an unrealistic amount of strain energy in the spring can be produced by a rigid body motion.

In a degenerated shell, the rotation of the normal and the mid-surface displacement field are independent. The idea then is to derive an additional constraint between the torsional rotation of the normal, α_3' , and the rotation of the mid-surface, $1/2(\partial w_2/\partial z_1 - \partial w_1/\partial z_2)$.

The deviation of the associated rotation from the mid-surface slope, Figure 3(a), is governed by the transverse shear strain energy, i.e.,

$$\pi_s = \kappa_s \mu h \int_S [\alpha_2'(r,s) + \frac{\partial w_3}{\partial z_1}(r,s,0)]^2 dA \quad (33)$$

In fact, the transverse shear stiffness K_s of Equation 20 can be obtained directly from the stationary value of π_s . Similarly, the deviation of the torsional rotation of the normal from that of the mid-surface, Figure 3(b), is assumed to have a governing strain energy,

$$\pi_t = \kappa_t \mu h \int_S [\alpha_3'(r,s) - \frac{1}{2} \{ \frac{\partial w_2}{\partial z_1}(r,s,0) - \frac{\partial w_1}{\partial z_2}(r,s,0) \}]^2 dA \quad (34)$$

where κ_t is a parameter to be determined. If $\kappa_t \mu h$ is chosen to be large relative to the factor $E h^3$ (which appears in the bending energy), Equation 34 will play the role of penalty function and results in the desired constraint:

$$\alpha_3' \approx \frac{1}{2} [\frac{\partial w_2}{\partial z_1} - \frac{\partial w_1}{\partial z_2}] \quad (35)$$

at the Gauss points. A one-point numerical integration should be used in evaluating the penalty integral in order to avoid an over-constrained situation similar to shear locking.

To derive a torsional stiffness from Equation 34, the local variables are expressed in terms of global nodal variables, δ^I , by bilinear shape functions. This gives Equation 34 in the form,

$$\pi_t = (\delta^I)^T K_t^{IJ} \delta^J \quad (36)$$

where the torsional stiffness,

$$K_t^{IJ} = \kappa_t \mu h \int_{-1}^1 \int_{-1}^1 \begin{bmatrix} (\mathbf{R}_m^I)^T \mathbf{R}_m^J & (\mathbf{R}_m^I)^T \mathbf{R}_n^J \\ (\mathbf{R}_n^I)^T \mathbf{R}_m^J & (\mathbf{R}_n^I)^T \mathbf{R}_n^J \end{bmatrix} |J(r,s,0)| dr ds \quad (37)$$

and

$$\mathbf{R}_m^I = \frac{1}{2} [\sum_k \theta_{k2} N_{,x_k}^I \quad - \sum_k \theta_{k1} N_{,x_k}^I \quad 0] \Theta^T \quad (38)$$

$$\mathbf{R}_n^I = N^I [\theta_{13} \quad \theta_{23} \quad \theta_{33}] \quad (39)$$

Since two penalty functions are included in the thin shell situation, the penalty factors, $\kappa_s \mu h$ and $\kappa_t \mu h$, should have magnitude of the same order. The result displayed in Figure 5 indicates that the converged solution is insensitive to κ_t , as long as κ_t is large enough (>0.1) to sufficiently restrain the troublesome torsional modes. This insensitivity demonstrates that the addition of a torsional stiffness will not degrade the behavior of the system after the torsional effect is deleted.

All numerical examples in this study employ a value of $\kappa_t=10$. It should be noted that in example 2 when the real hyperbolic paraboloid shell geometry is exactly represented, an identical solution is obtained with or without the torsional stiffness.

NUMERICAL EXAMPLES

To demonstrate the effectiveness and the versatility of the element, several examples of different shell situations are analyzed.

Thin cylindrical shell roof: The thin cylindrical shell in Figure 4 is tested with meshes of 4, 16 and 64 elements. The shell is supported at both ends on rigid diaphragms. This example shows a situation where both membrane and bending actions are significant.

Initially the problem is solved without the addition of a torsional stiffness K_t . The solution fails to converge as is evident in Figure 6, graph 8. A parameter study of κ_t is then carried out for both thick and thin shells, using different element meshes. The results are displayed in Figure 5. The adding of the torsional stiffness with sufficient amount of κ_t to restrain the free torsional mode produces a unique and converged solution.

The convergence characteristics are compared with other elements in Figure 6. The present solution converges to a complete (non-shallow) shell solution. This is also true for many of the shell elements which possess no geometric slope continuity at the element boundaries [23]. The BDS element proves to be highly competitive --- only some of the higher order elements perform better for the same number of degrees of freedom. The bilinear element, however, requires much less time to formulate due to its simplicity.

Figures 7 and 8 compare displacements to shallow-shell exact solutions. The corresponding deep-shell solutions are not available. The stress-resultants are also shown to be very accurate in Figure 9.

Clamped hyperbolic paraboloid shell: In this example, Figure 10, the element assemblage exactly represents the real shell geometry. The shell is subjected to a uniform normal pressure. The deflection along the center is plotted in Figure 11 and compared to the exact solution reported in [19]. Figure 12 shows the rapid convergence of the solution compared to the relatively slow convergence in [14]. In that reference, the element was specially designed for the shallow hyper shell in which a cubic transverse displacement and linear inplane displacements were used.

Thick cylindrical shell: The problem consists of a long cylindrical shell of uniform thickness, Figure 13, resting on a line support and subjected to gravity loading. Figure 14 shows the deformed mid-surface which checks well with the simple ring analytical solution. In comparison solutions obtained by the 2-D plane-strain continuum element (Q-4) and the present element but with exact numerical integration are shown. As expected, they are both too stiff.

Arch dam: This example provides a good test of the element in the case of an arbitrary, thick shell with varying thickness. Figure 15 shows a doubly curved arch dam known to be type 5 [15,16]. Details of the geometry can be found in [15] and [16]. In Figure 16, the down stream displacement is plotted and compared with the solutions from a thin shell element, a 3-D continuum element, and a higher-order element [12].

It is remarkable to note that accurate results are attainable with a very crude mesh (16 elements) using this low order element, and are comparable to those of the finer mesh (32 elements) using the higher-order element of [12].

Curved box girder: The last example shows a more complex structure of a curved box girder as detailed in Figure 17. The present element is used for the flanges, curved webs and diaphragm

of the box girder. For webs, a 1-by-2 Gaussian quadrature, Figure 18, is employed for the inplane μ -energy term to avoid the poor beam-bending behavior which is analogous to the transverse shear-locking in the shell situation. The 2-point integration along the web thickness is necessary to include the equivalent effect of the analytical integration in a classical beam. The diaphragm is treated as a membrane by deleting the bending stiffness.

The vertical deflection and normal stresses in both flanges are plotted in Figures 19,20 and 21. The solutions are compared with both the experiment and the higher-order finite-element solutions reported in [17]. The present element proves to perform surprisingly well in all aspects.

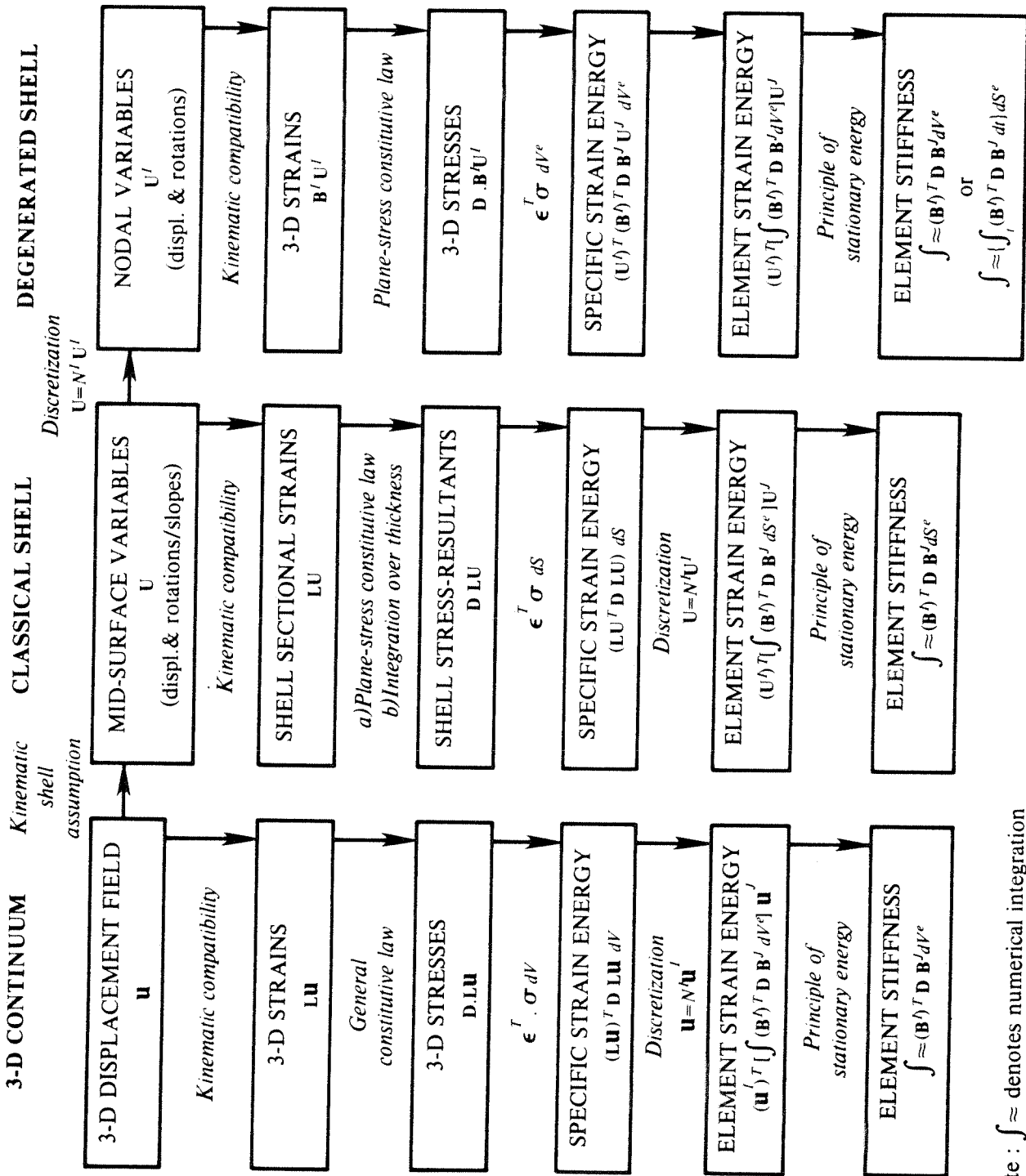
CONCLUSIONS

The attractiveness of the BDS element is attributed to its efficiency, effectiveness and versatility. The simplest element geometry is chosen so that the element can serve as a convenient basis for unlimited forms of shell geometry. The degeneration concept, coupled with a reduced integration technique, produces a shell element which performs accurately in both thick and thin shell situations. With slight modification, the element is also capable of analyzing other types of thin structures, such as a curved web of the curved box girder.

REFERENCES

- [1] S.F. Pawsey, 'The analysis of moderately thick to thin shells by the finite element method,' SESM Report No. 70-12, Dept. of Civil Engineering, U.C. Berkeley, August 1970.
- [2] H.H. Dovey, 'Extension of three dimensional analysis to shell structures using the finite element idealization,' SESM Report No. 74-2, Dept. of Civil Engineering, U.C. Berkeley, January 1974.
- [3] T.J.R. Hughes, R.L. Taylor and W. Kanoknukulchai, 'A simple and efficient finite element for plate bending', *Int.J.num.Meth.Engng.*, 11,1529-1543(1977).
- [4] E.L. Wilson, R.L. Taylor, W.P. Doherty and J. Ghaboussi, 'Incompatible displacement models', *Numerical and Computer Methods in Structural Mechanics*, ed. S.J. Fenves et.al., Academic Press, New York (1973).
- [5] R.W. Clough and R.J. Johnson, 'A finite element approximation for the analysis of thin shell', *Int.J.Solids Struct.*, 4,43-60(1968).
- [6] S.W. Key and Z.E. Beisinger, 'The analysis of thin shells with transverse shear strains by the finite element method', *Proc. Conf.Matrix Meth.Struct.Mech. Wright-Patterson Air Force Base, Ohio*, AFFDL-TR-68-150, 667-710(1968).
- [7] B.M. Irons and K.J. Draper, 'Inadequacy of nodal connections in stiffness solution for plate bending', *AIAA J.* 3,5,965(1965).
- [8] R.J. Melosh, 'A flat triangular shell element stiffness matrix', *Proc.Conf.Matrix Meth.Struct.Mech., Wright-Patterson Air Force Base, Ohio*, AFFDL-TR-66-80, 503-514(1965).
- [9] S. Utku, 'Stiffness matrices for thin triangular elements of non-zero Gaussian curvature', *AIAA J.* 5,9,1659-1667(1967).
- [10] G.A. Wempner, J.T. Oden and D.A. Kross, 'Finite-element analysis of thin shell', *J.Engng.Mech.Div. ASCE* 94,EM6,1273-1293(1968).
- [11] O.C. Zienkiewicz, R.L. Taylor and J.M. Too, 'Reduced integration technique in general analysis of plates and shells', *Int.J.num.Meth.Engng* ,3,275-290(1971).
- [12] S. Ahmad, B.M. Irons and O.C. Zienkiewicz, 'Analysis of thick and thin shell structures by curved finite elements', *Int.J.num.Meth.Engng.* ,2,419-451(1970).
- [13] O.C. Zienkiewicz and E. Hinton, 'Reduced integration, function smoothing and non-conformity in finite element analysis', *J.Franklyn Inst.* 302,443-461(1976).
- [14] J.J. Connor and C. Brebbia, 'Stiffness matrix for shallow rectangular shell element', *J.Engng.Mech.Div. ASCE* 93,EM5,43-65(1967).
- [15] J. Ergataudis, B.M. Irons and O.C. Zienkiewicz, 'Three-dimensional analysis of arch dams and their foundations', *Proc.Symp.Arch dams Inst. civ. Engng.*, London, 37-50(1968).
- [16] O.C. Zienkiewicz, C.J. Parekh and I.P. King, 'Arc dams analyzed by a linear finite element solution program', *Proc.Symp.Arch dams Inst.civ.Engng.*, London,19-23(1968).
- [17] A.R.M. Fam and C. Turkstra, 'Model study of horizontally curved box girder', *J.Engng.Str.Div.* ,ASCE 102,ST5,1097-1108(1976).
- [18] A.C. Scordelis and K.S. Lo, 'Computer analysis of cylindrical shells', *ACI J.* 61,1,539-561(1964).
- [19] S. Chetty and H. Tottenham, 'An investigation into the bending analysis of hyperbolic paraboloid shells', *Indian Concrete Journal* ,July,1964.

- [20] O.C. Zienkiewicz, *The Finite Element Method*, McGraw-Hill, London (1977).
 - [21] G.R. Cowper, G.M. Lindberg and M.D. Olson, 'A shallow shell finite element of triangular shape', *Int.J. Solids Struct.* 6, 1133-1156 (1970).
 - [22] R.L. Taylor, *private communications*.
 - [23] K. Forsberg, *An Evaluation of Finite Difference and Finite Element Techniques for Analysis of General Shells*, Symposium on high speed computing for elastic structures, IUTAM, Mechanics, Liege, 1970.
-



Note : $\int \approx$ denotes numerical integration

Figure 1. Strategies of shell element derivation.

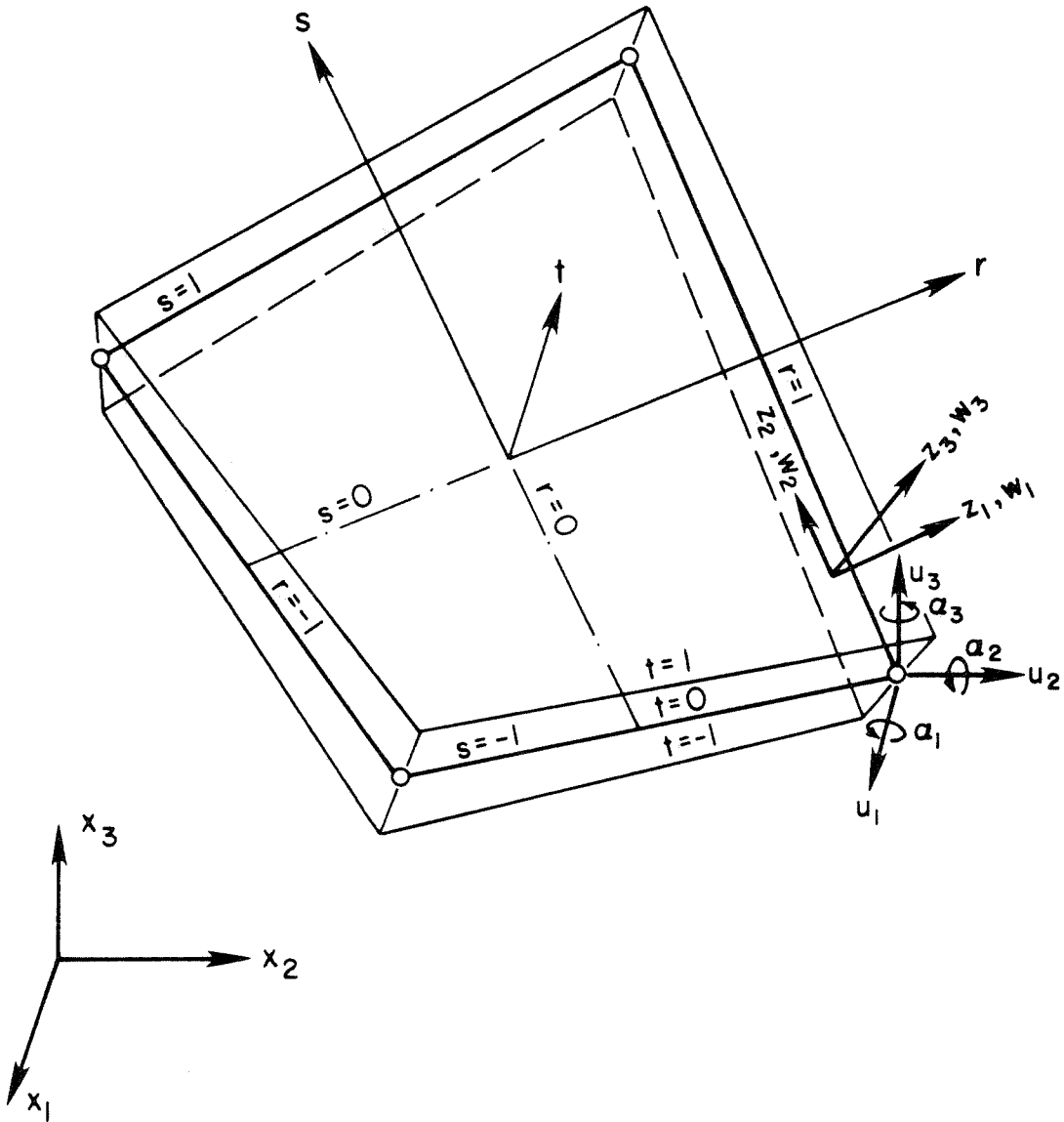


Figure 2. Bilinear shell element.

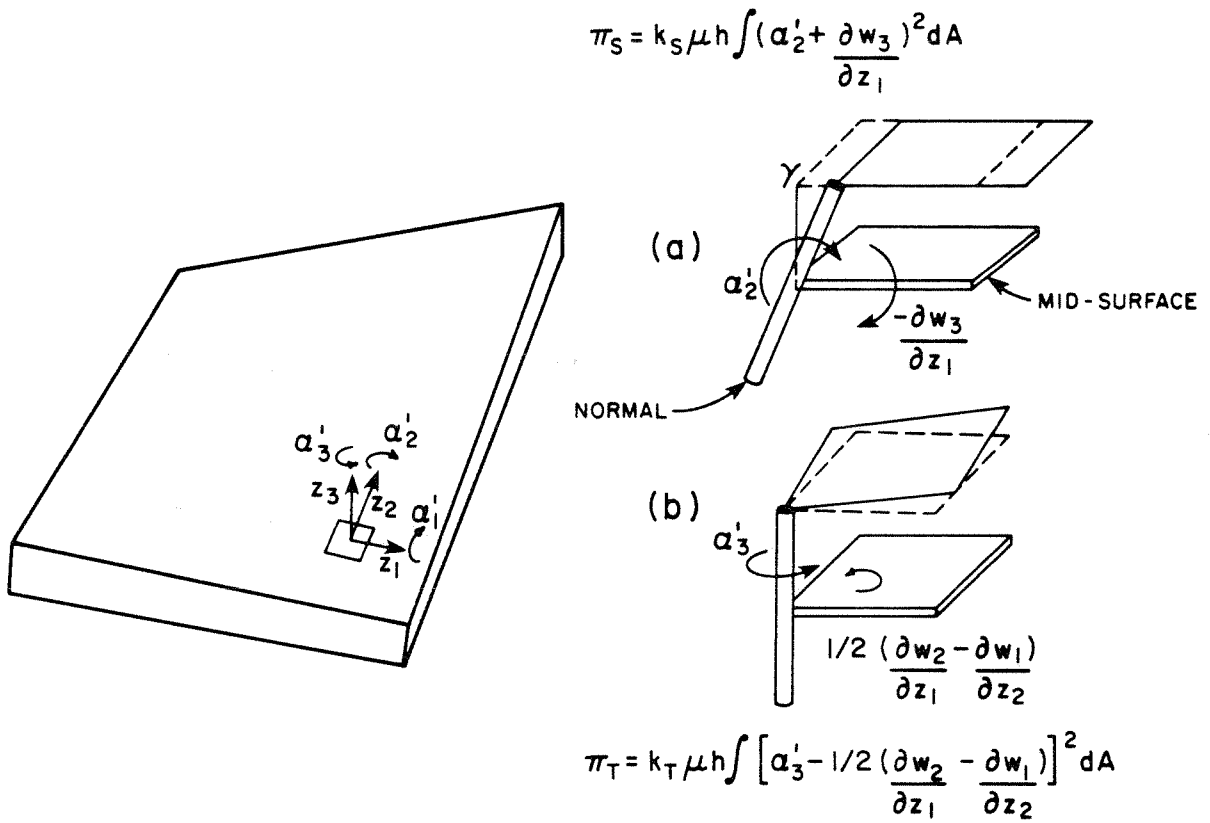


Figure 3. Penalty functions: (a) transverse shear (b) torsion.

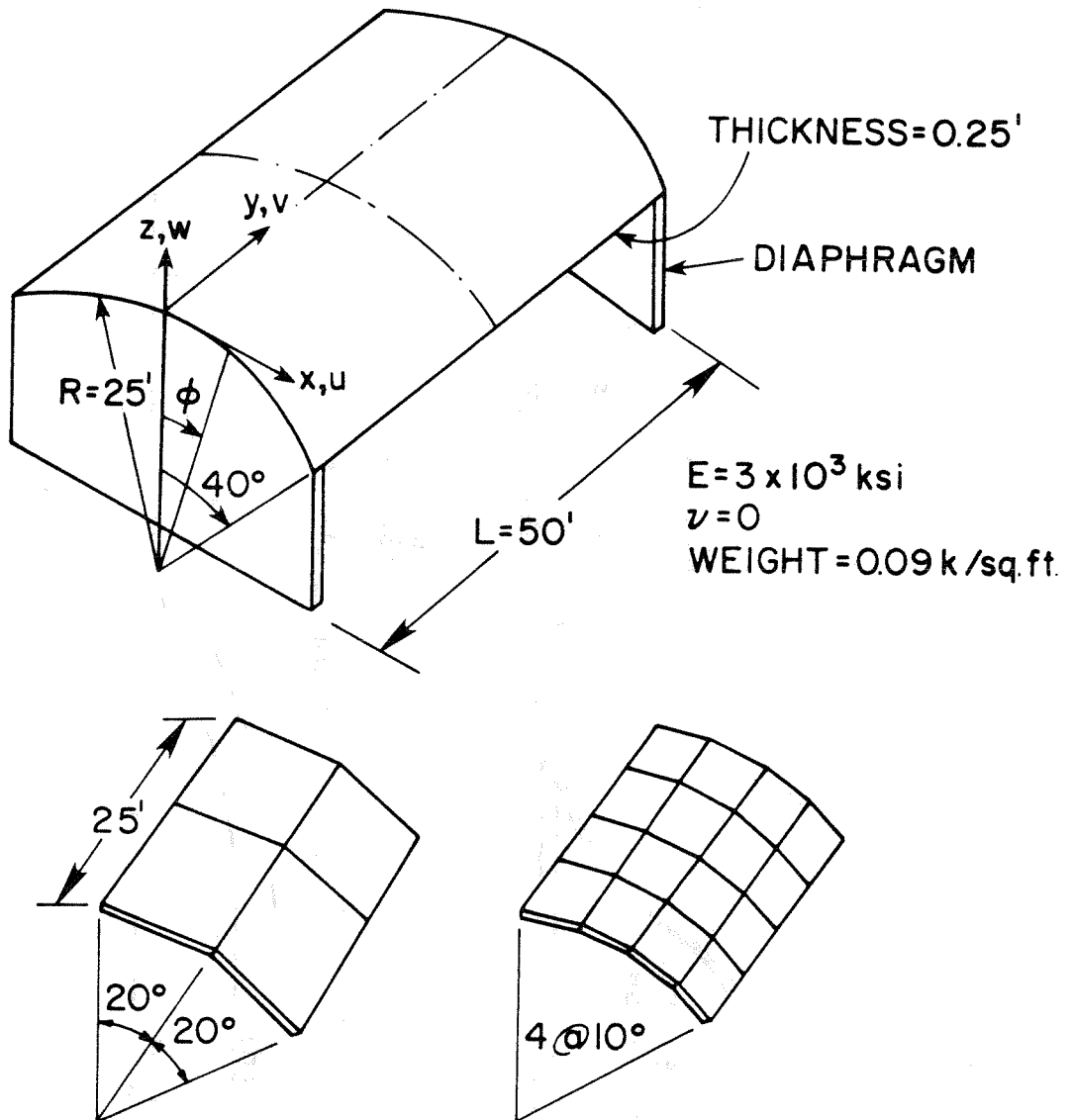


Figure 4. Thin cylindrical shell. Geometry and meshes of 4 and 16 elements.

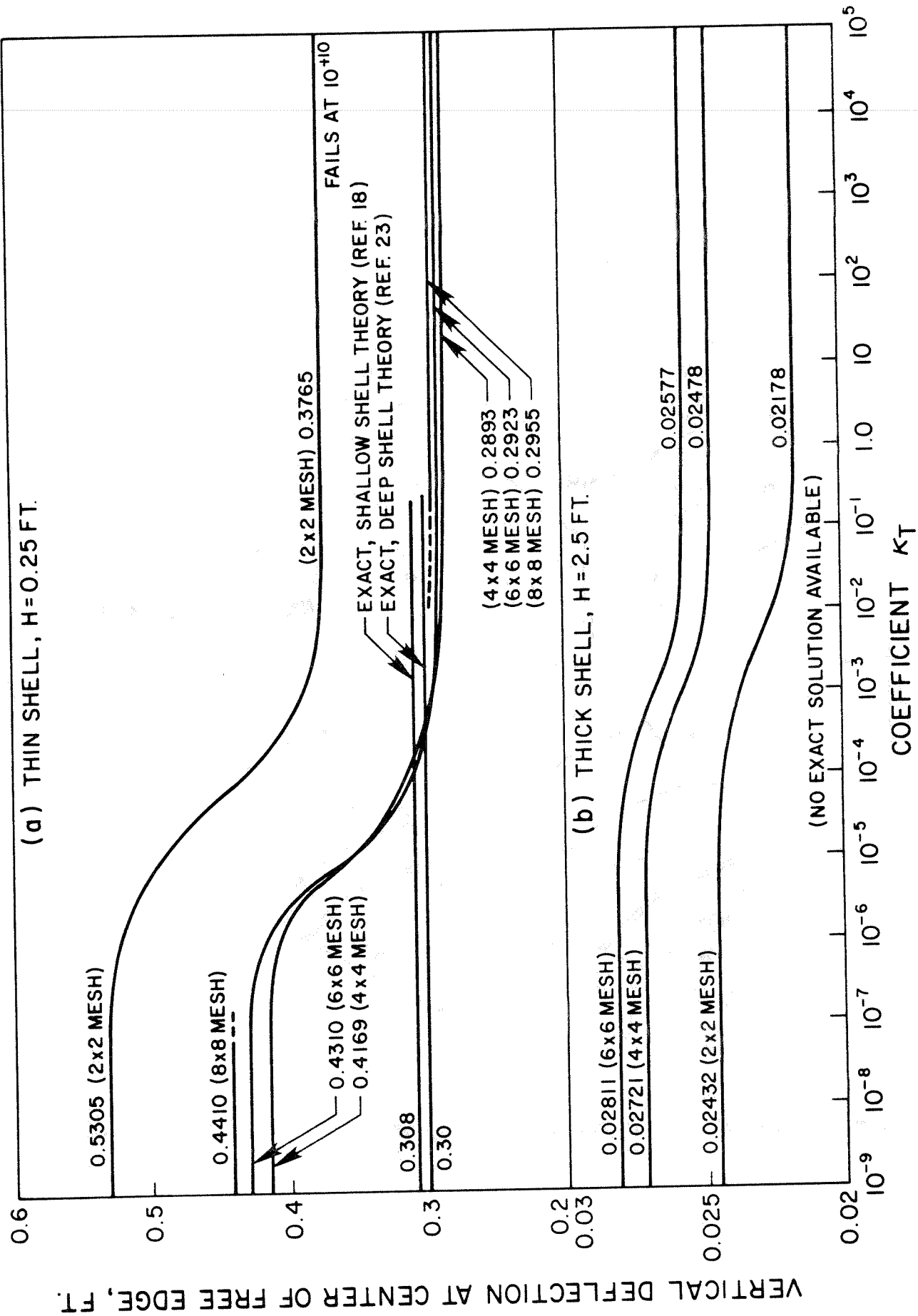


Figure 5. Effect of torsional stiffness to solutions of thin and thick cylindrical shell roofs.

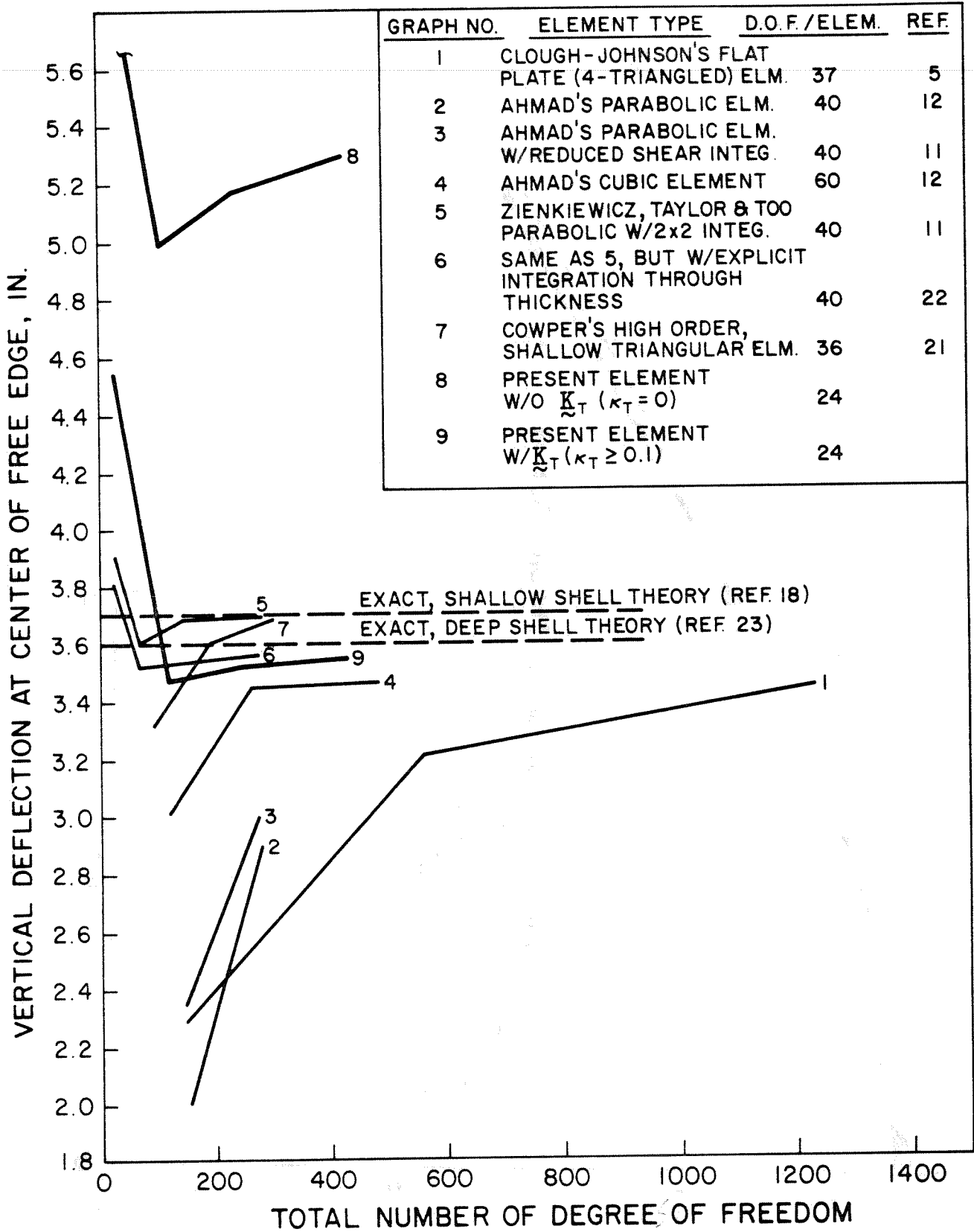


Figure 6. Convergence of deflection versus degrees of freedom, thin cylindrical shell roofs.

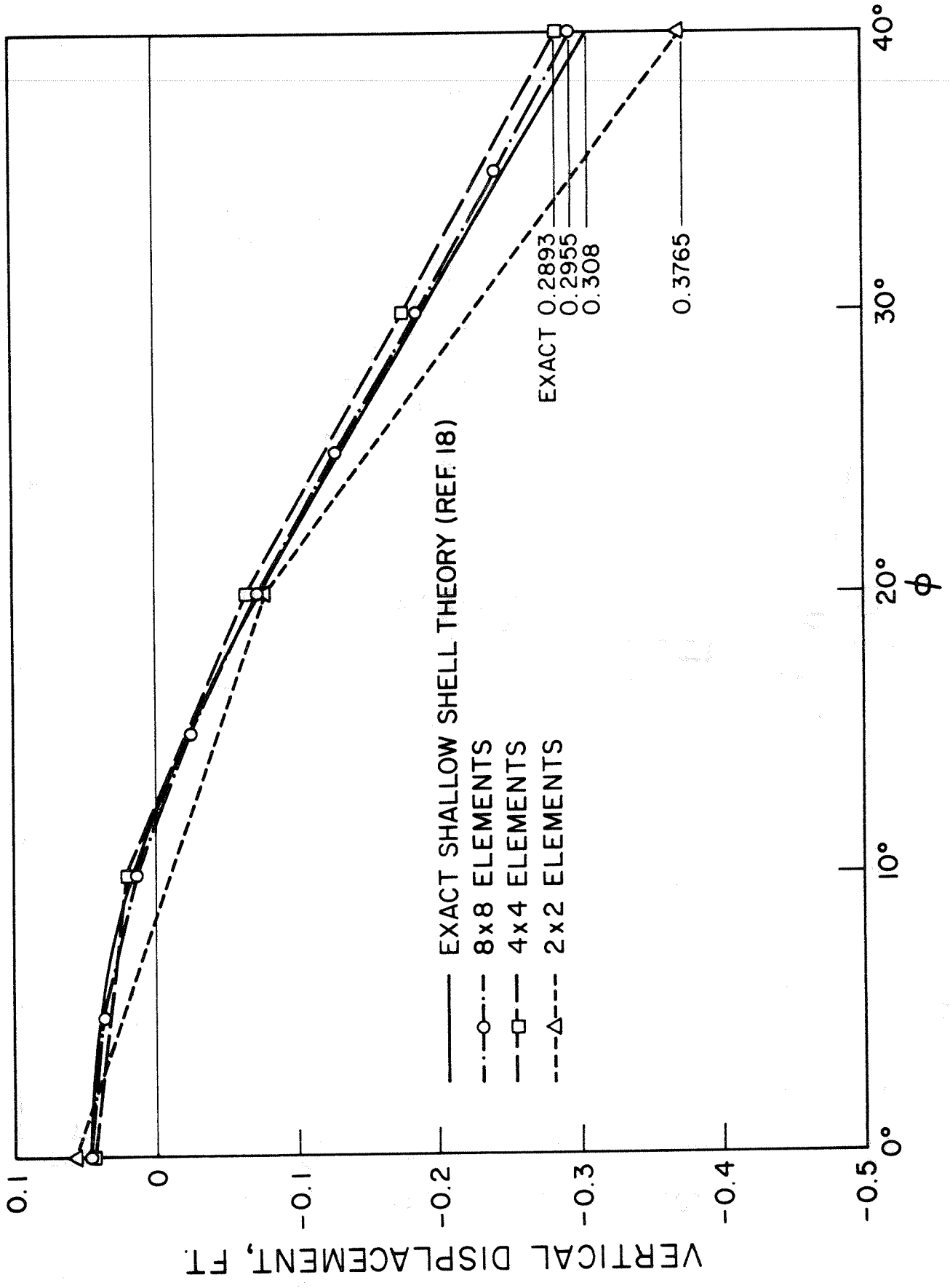


Figure 7. Cylindrical shell roof, vertical displacement at $y = 1/2$.

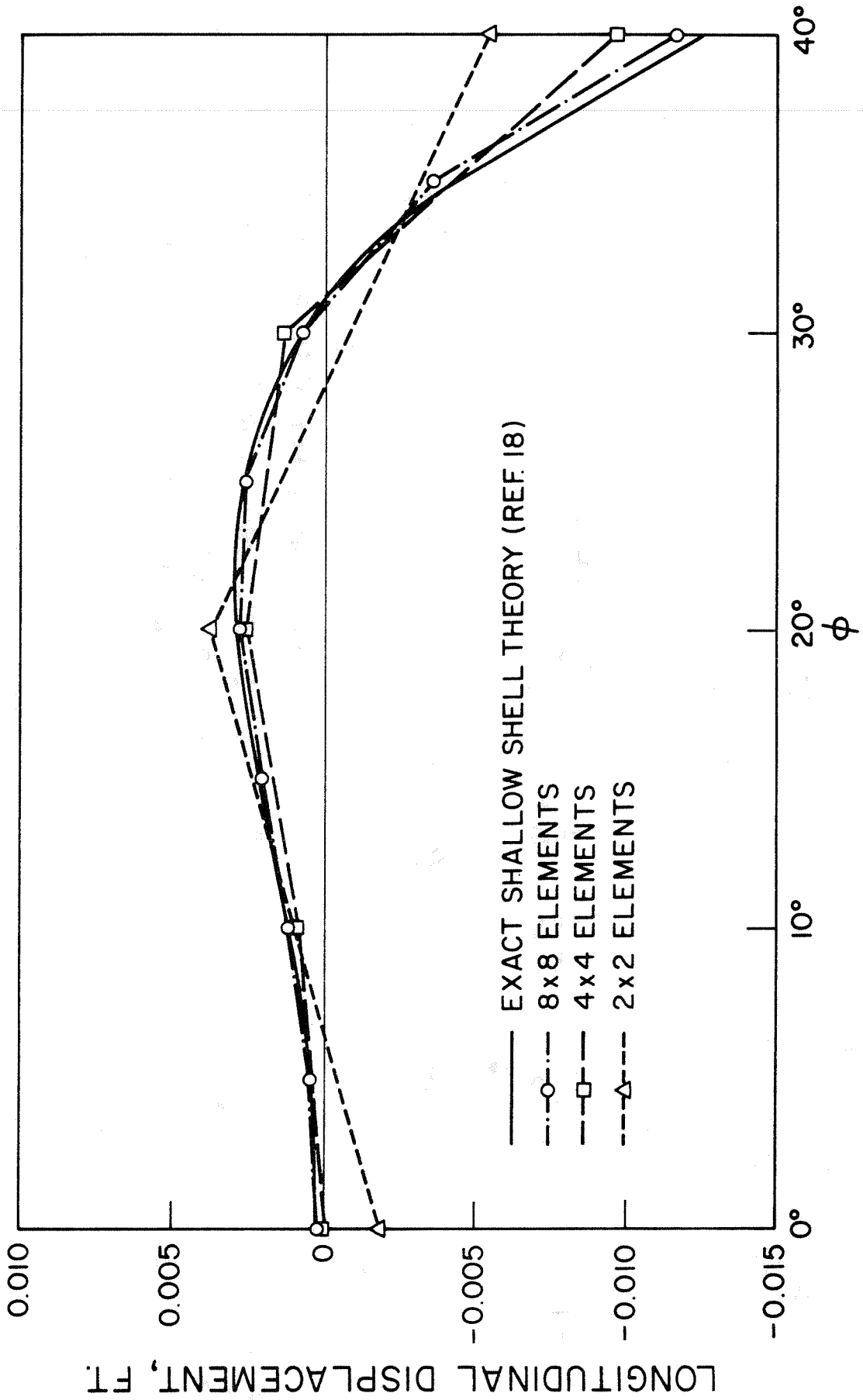
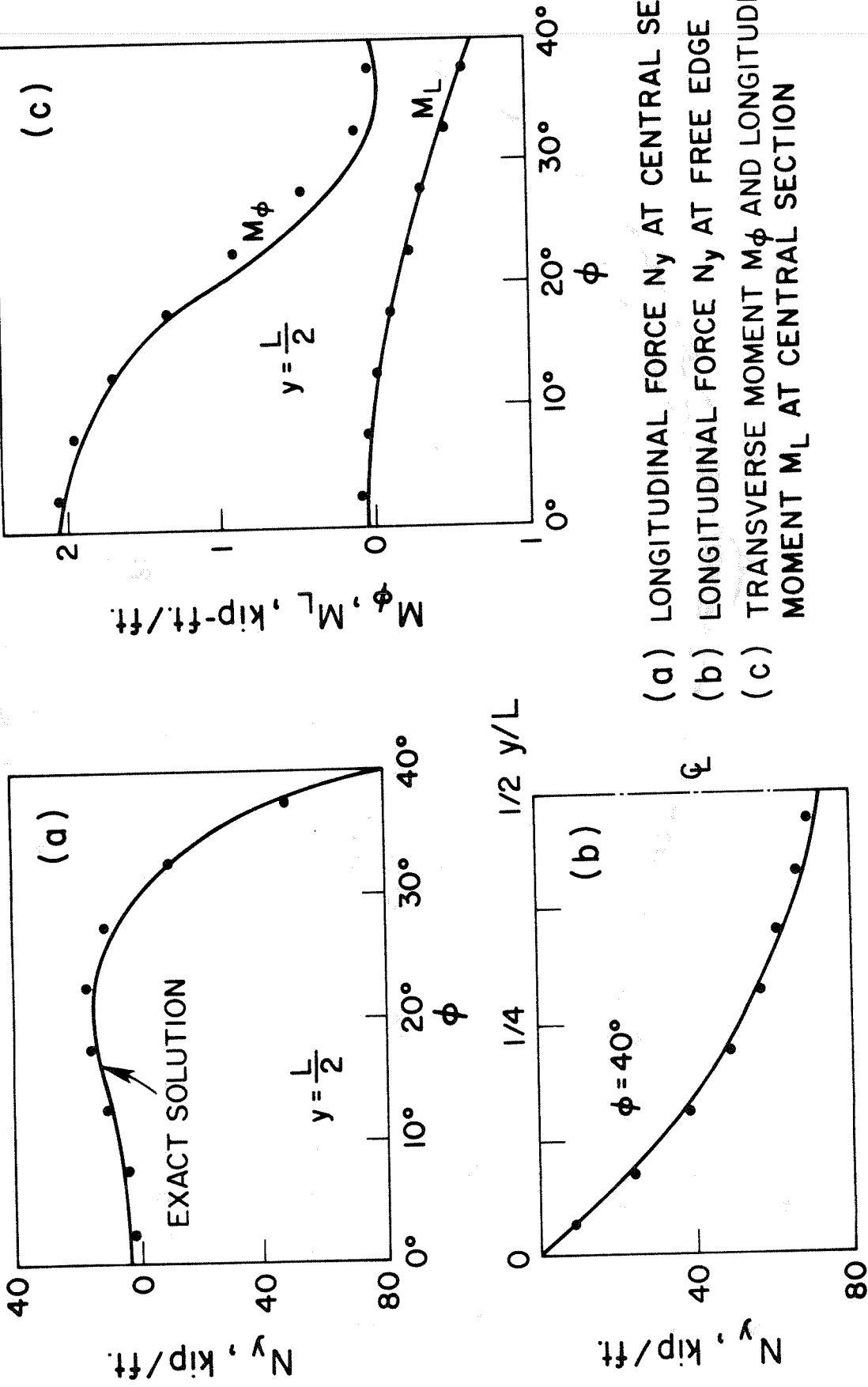


Figure 8. Cylindrical shell roof, longitudinal displacement at diaphragm ($y = 0$).



(a) LONGITUDINAL FORCE N_y AT CENTRAL SECTION
 (b) LONGITUDINAL FORCE N_y AT FREE EDGE
 (c) TRANSVERSE MOMENT M_ϕ AND LONGITUDINAL MOMENT M_L AT CENTRAL SECTION

Figure 9. Stress resultants for 8-by-8 element mesh. All stresses are obtained by the interpolation of values at Gauss points.

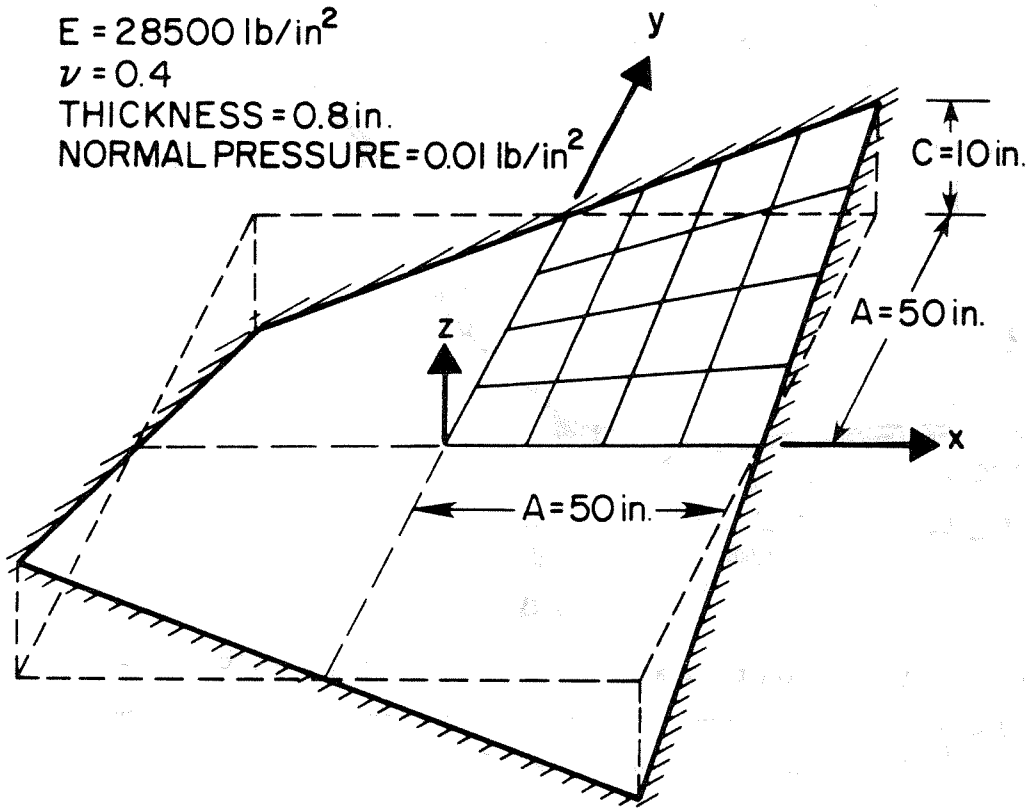


Figure 10. Clamped hyperbolic shell.

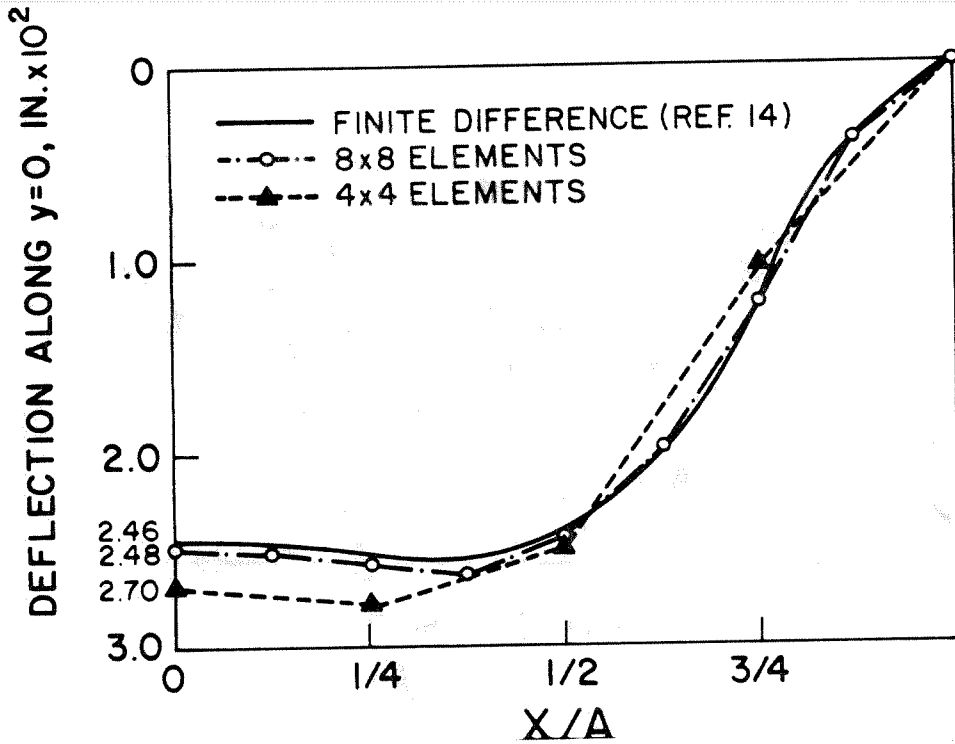


Figure 11. Deflection at center line of hyperbolic shell.

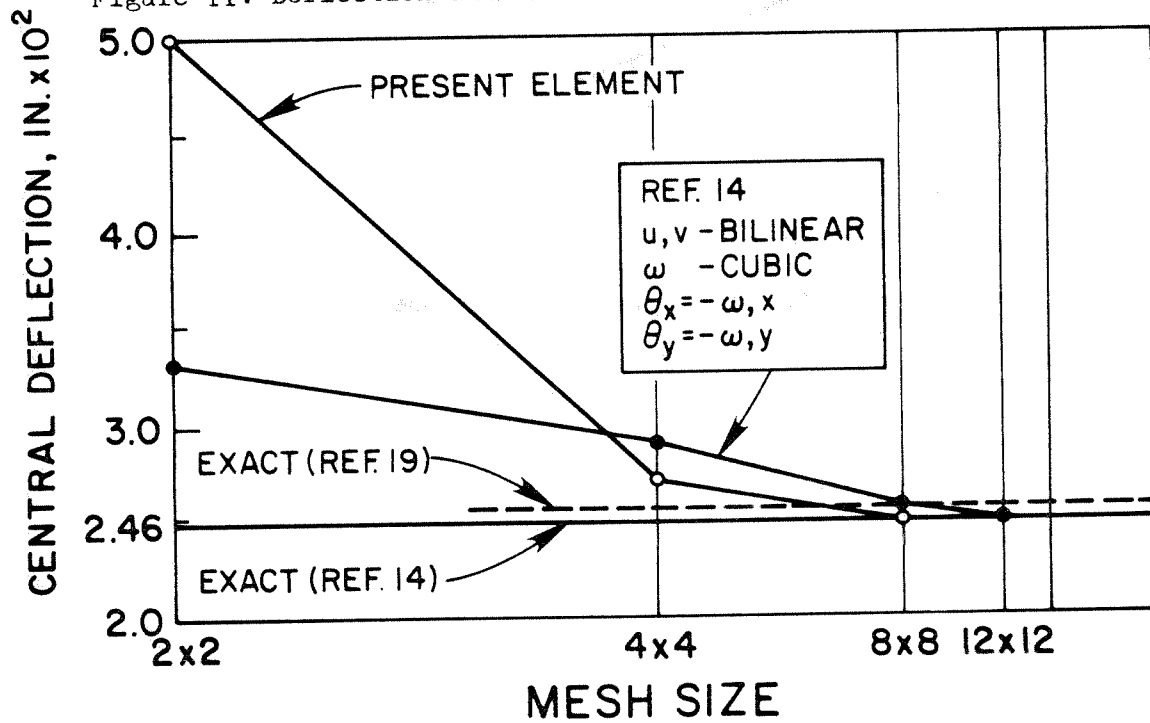


Figure 12. Clamped hyperbolic shell, convergence of central deflection.

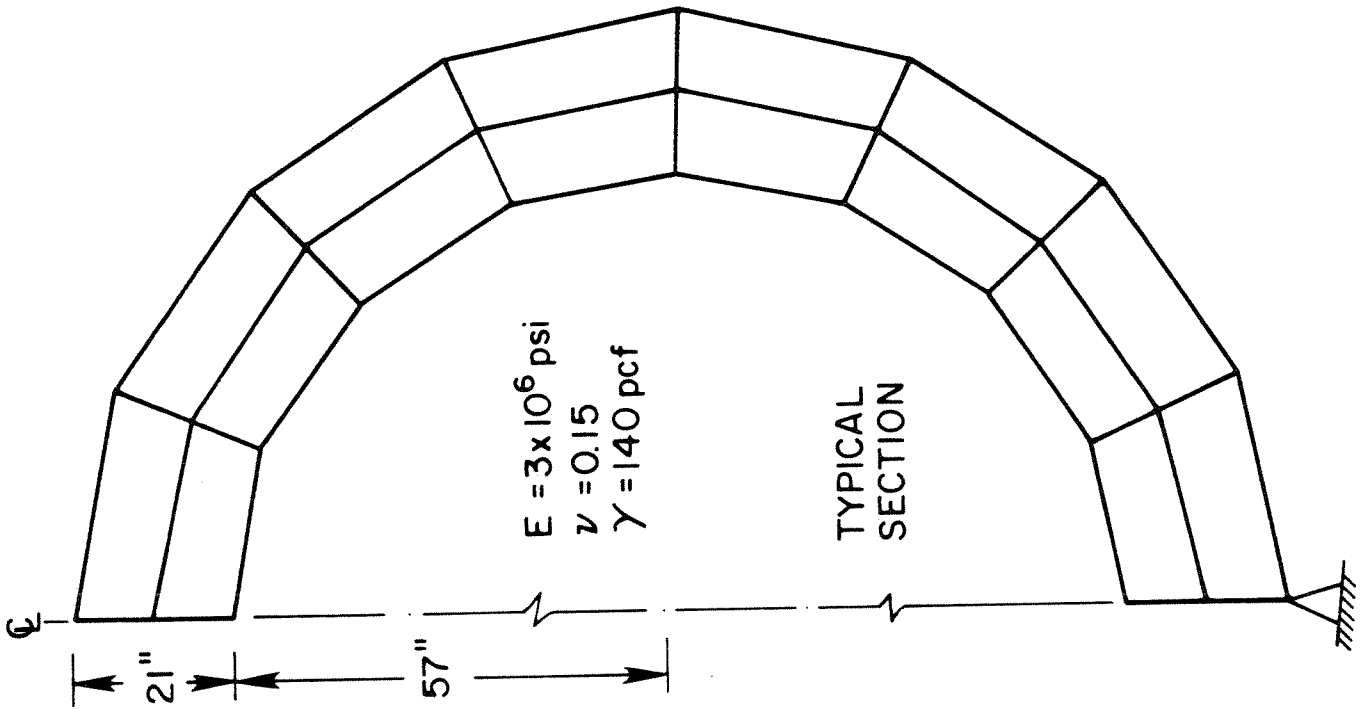


Figure 13. Long cylindrical thick shell on line support.

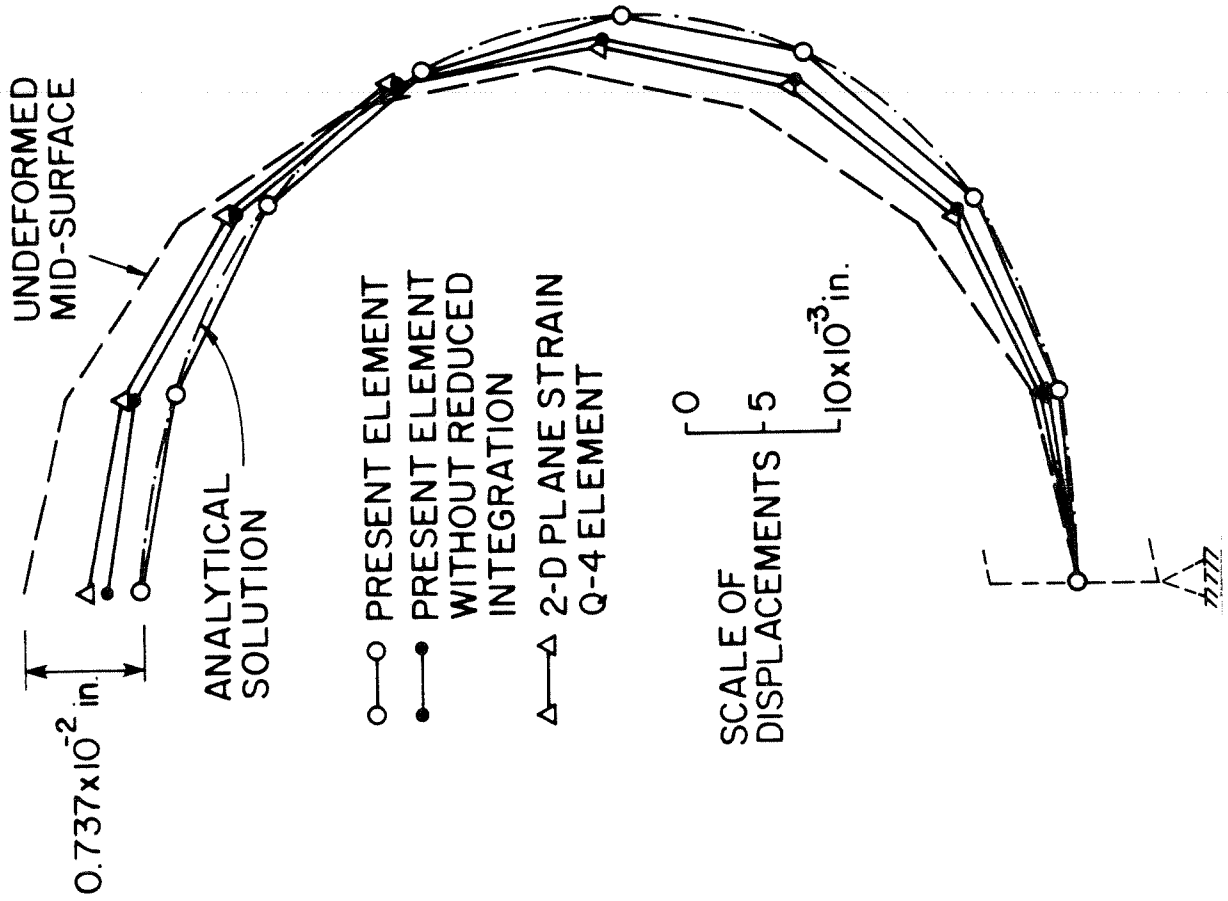


Figure 14. Deformed mid-surface of cylindrical shell due to gravity loading.

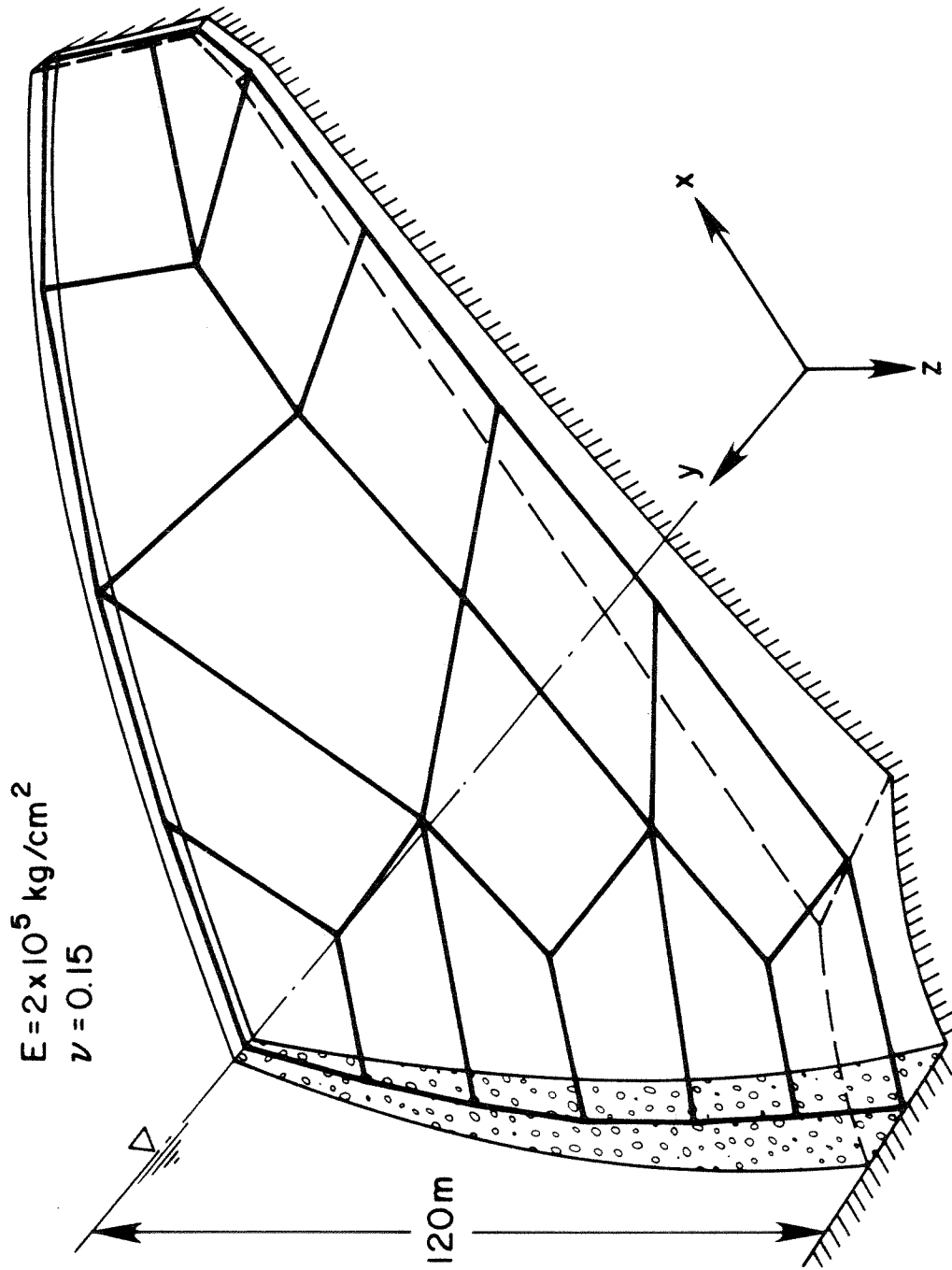


Figure 15. Arch dam type 5, 16-element mesh.

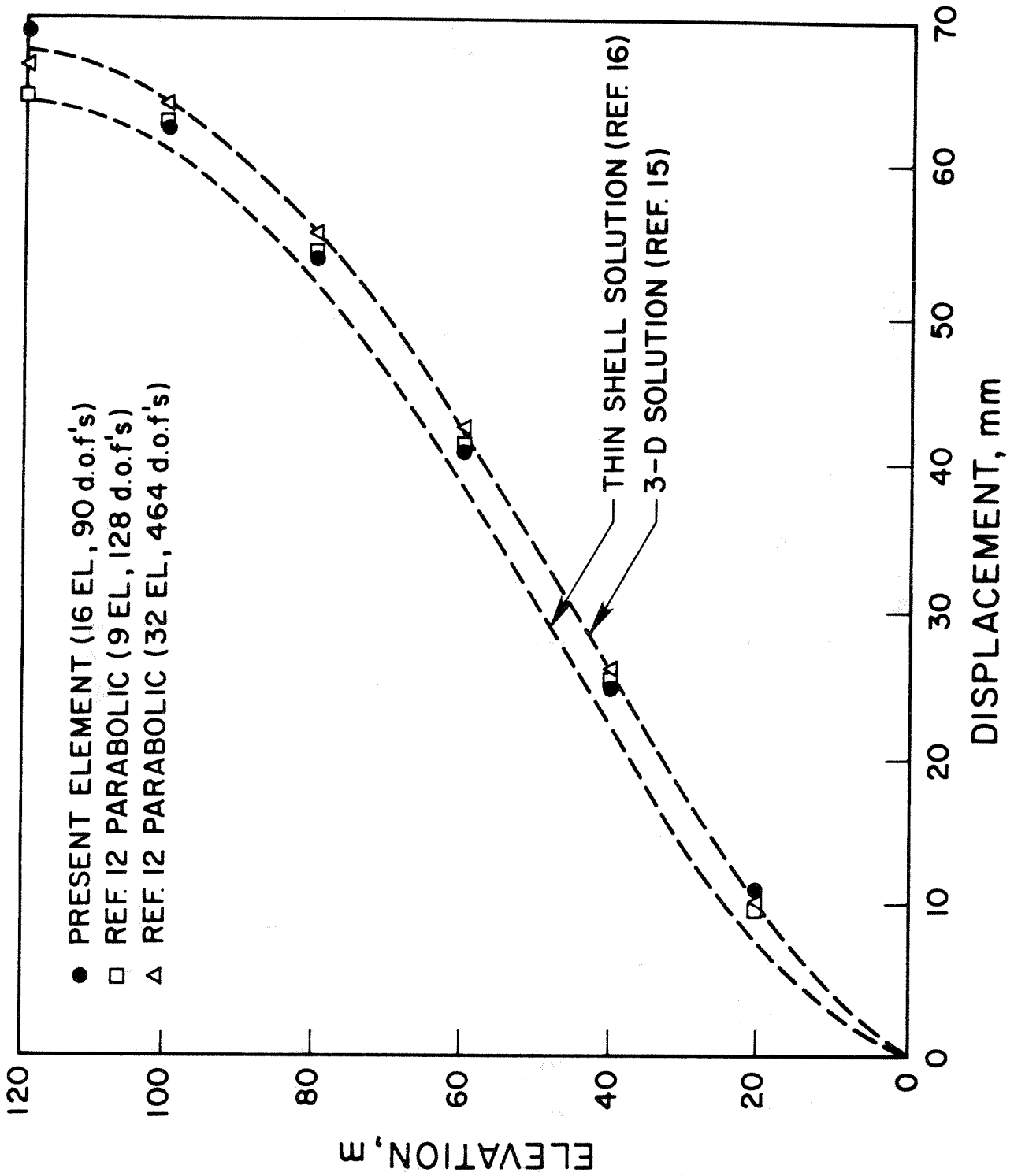
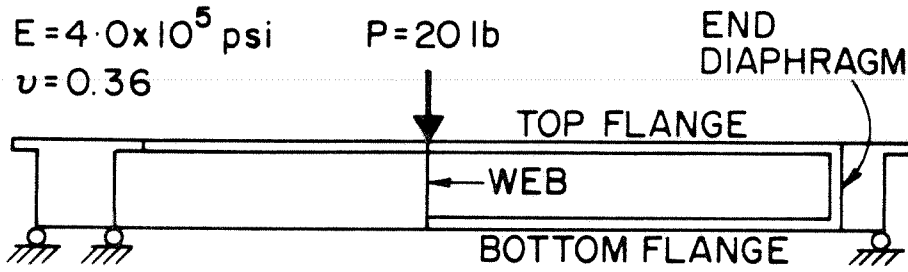
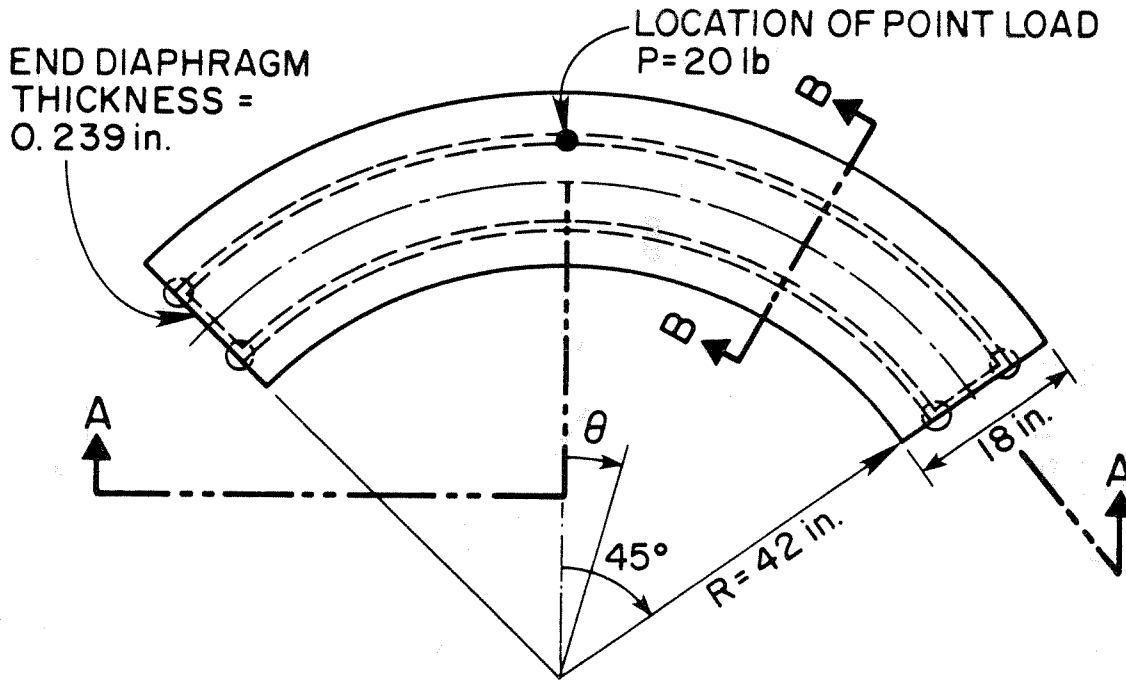


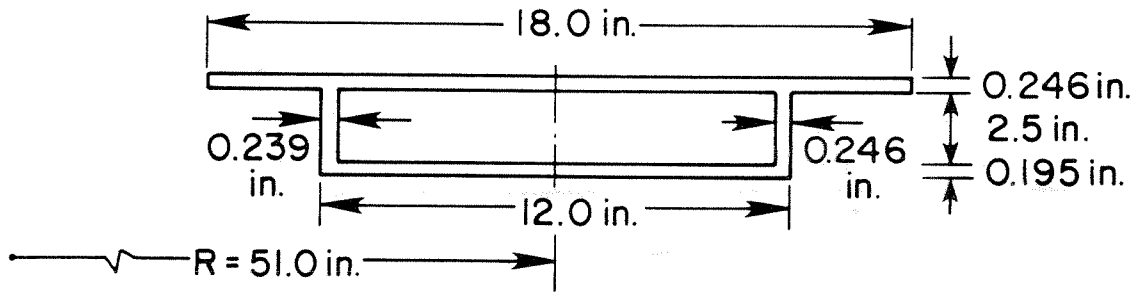
Figure 16. Downstream displacements on crown section of dam type 5.



(a) SECTION A-A

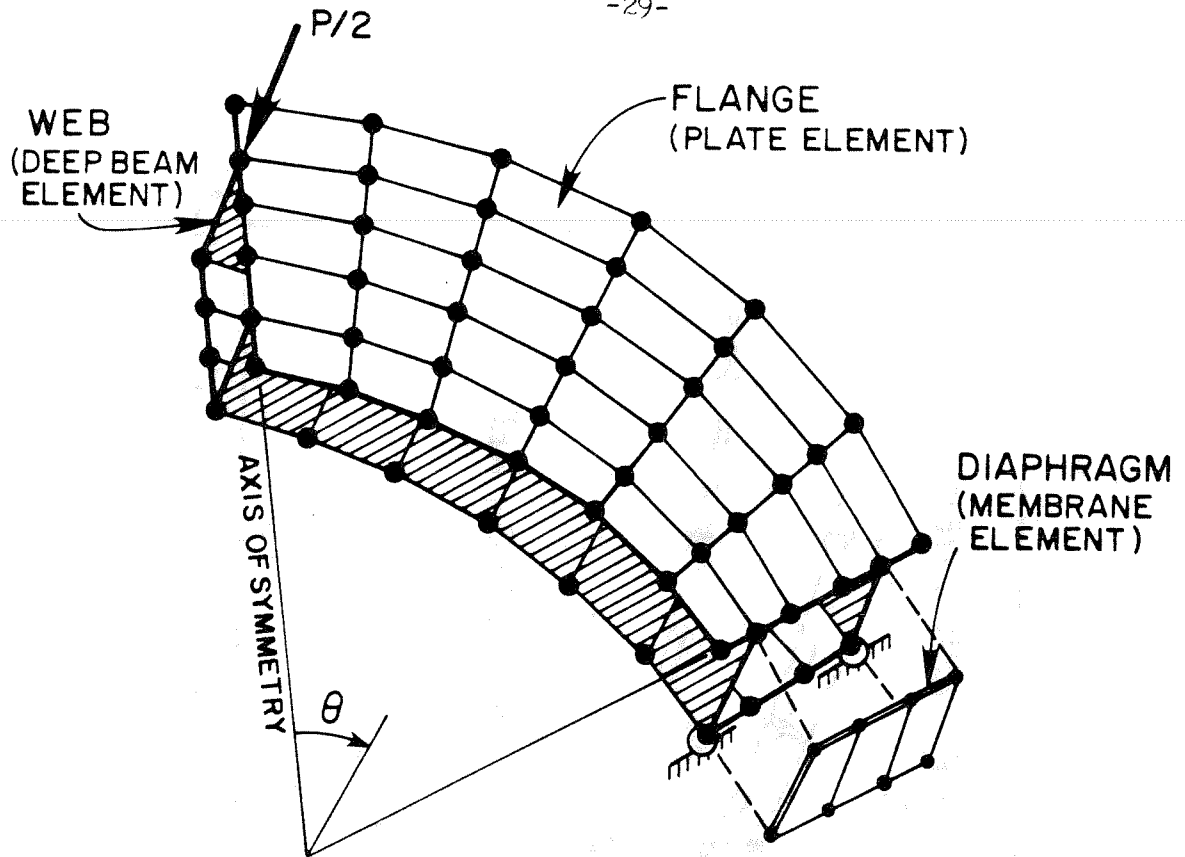


(b) TOP VIEW



(c) SECTION B-B

Figure 17. A horizontally curved box girder.



(a) FINITE ELEMENT MESH

TYPE	DOMINANT ACTION	GAUSSIAN QUADRATURE		
		NORMAL STRESSES	IN-PLANE SHEAR	TRAVERSE SHEAR
FLANGE (PRESENT ELEMENT)		 2x2	 2x2	 1x1
WEB (PRESENT ELEMENT W/ IN-PLANE SHEAR MODIFICATION)		 2x2	 2x1	 1x1
DIAPHRAGM (PRESENT ELEMENT W/ OUT-OF-PLANE EFFECT NEGLECTED)		ALL 2x2 OUT-OF-PLANE EFFECT IGNORED		

(b) MODIFICATION OF THE ELEMENT FOR WEB MEMBERS AND DIAPHRAGM

Figure 18. Curved box girder, finite element idealization.

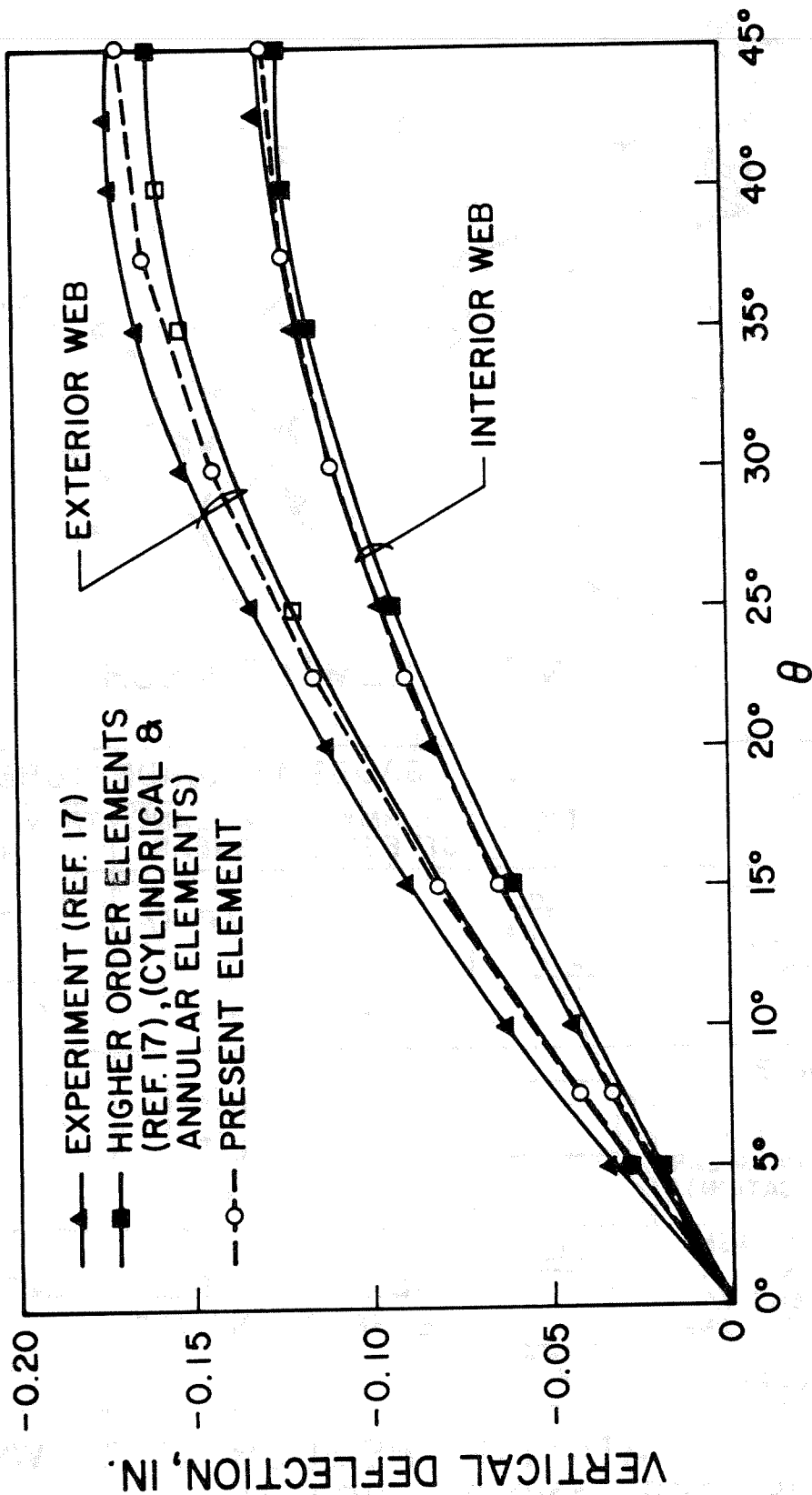


Figure 19. Vertical deflection along half span of box girder.

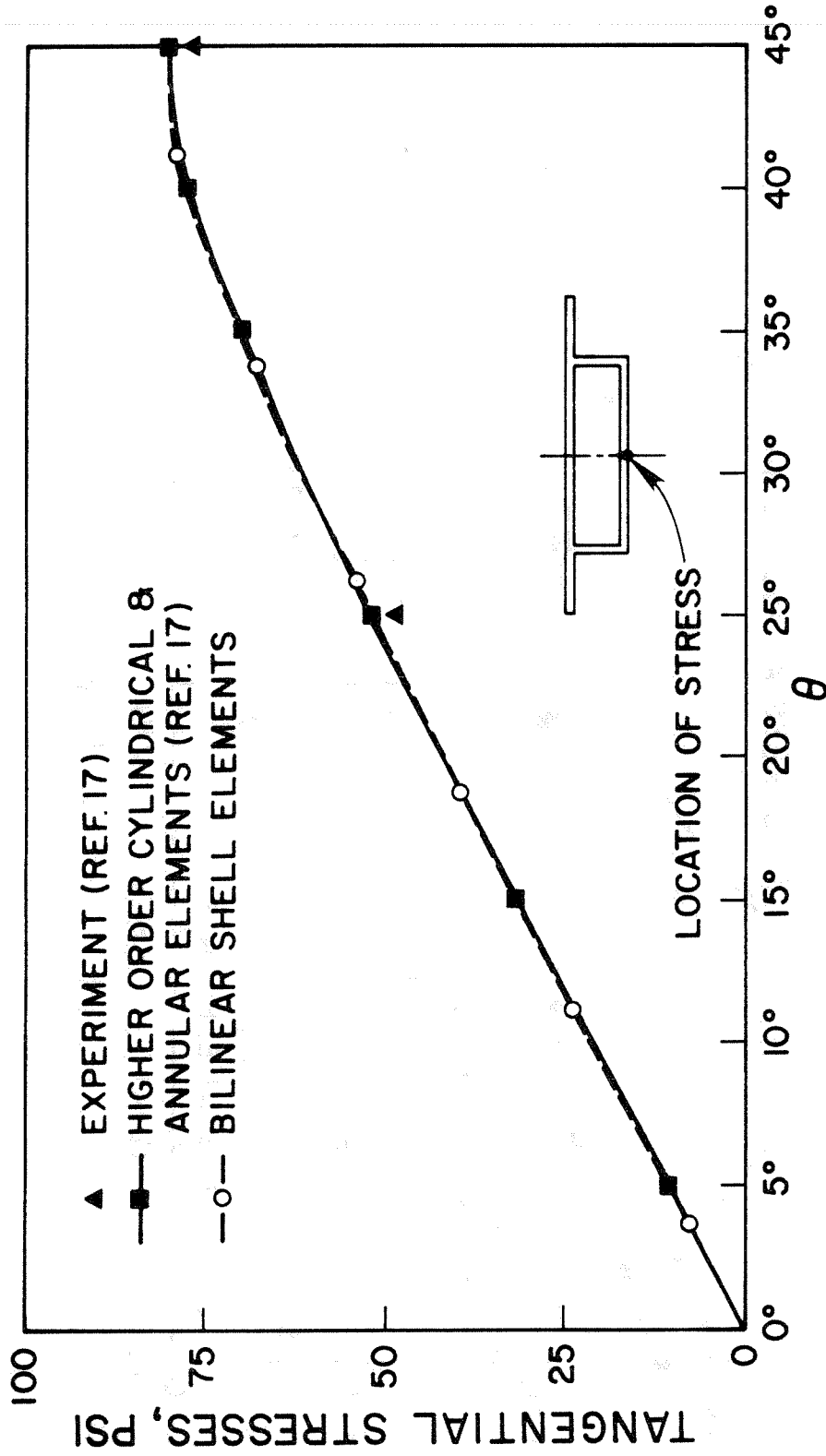


Figure 20. Tangential stresses on outer face of the bottom flange of box girder.

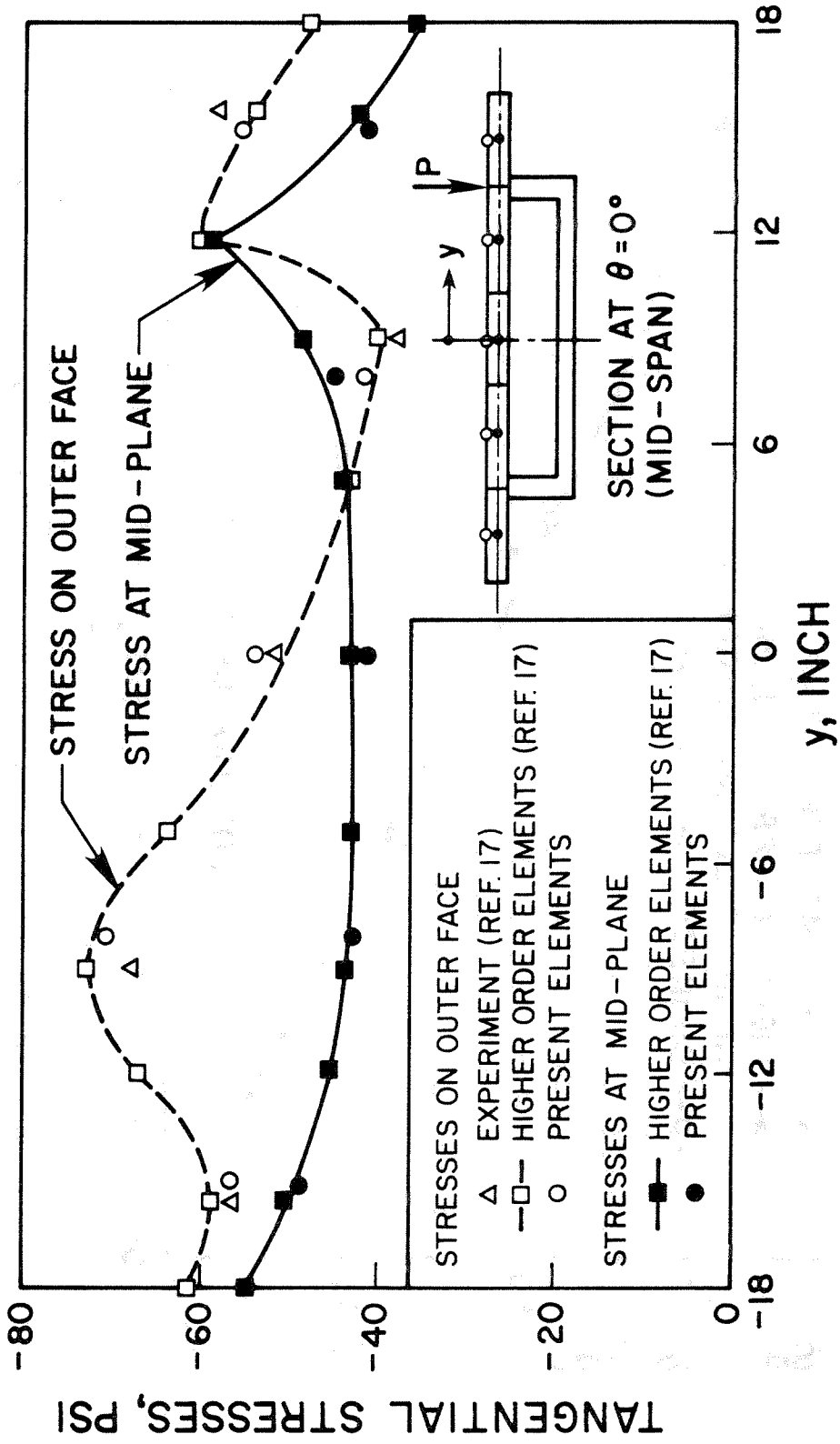


Figure 21. Tangential stresses in top flange at mid-span of box girder.

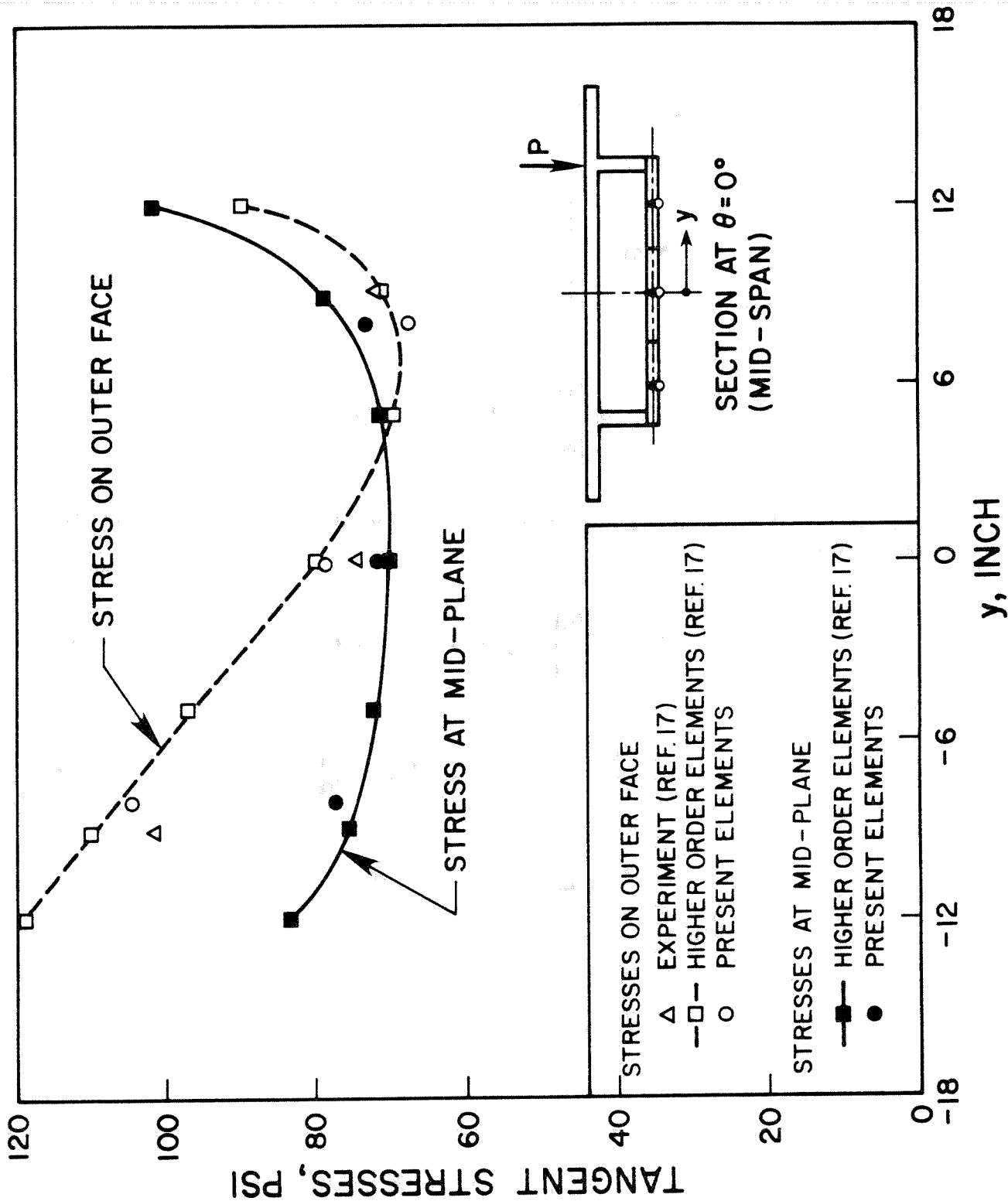


Figure 22. Tangential stresses in bottom flange at mid-span of box girder.

APPENDIX A

Shell Stress-Resultants

The usual shell stress-resultants: membrane forces, shears and couples, are defined as follows

$$\mathbf{N}(r,s) \equiv \begin{Bmatrix} N_{11} \\ N_{22} \\ N_{12} \\ N_{13} \\ N_{23} \end{Bmatrix} = \int_{-h/2}^{h/2} \boldsymbol{\sigma}(r,s,t) dz_3 \quad (\text{A1})$$

$$\mathbf{M}(r,s) \equiv \begin{Bmatrix} M_{11} \\ M_{22} \\ M_{12} \end{Bmatrix} = \int_{-h/2}^{h/2} z_3 \boldsymbol{\sigma}(r,s,t) dz_3 \quad (\text{A2})$$

The equation (24) is substituted in (14) and the result in (A1) and (A2) which are then integrated to yield

$$\mathbf{N}_m \equiv \begin{Bmatrix} N_{11} \\ N_{22} \\ N_{12} \end{Bmatrix} = \sum_I h(r,s) \mathbf{D}_m \mathbf{B}_{1m}^I \mathbf{u}^I \quad (\text{A3})$$

$$\mathbf{N}_s \equiv \begin{Bmatrix} N_{13} \\ N_{23} \end{Bmatrix} = \sum_I h(r,s) \mathbf{D}_s [\mathbf{B}_{1s}^I \mathbf{B}_{2s}^I] \begin{Bmatrix} \mathbf{u}^I \\ \boldsymbol{\alpha}^I \end{Bmatrix} \quad (\text{A4})$$

$$\mathbf{M} = \sum_I \frac{h^2}{6}(r,s) \mathbf{D}_m \mathbf{B}_{3m}^I \boldsymbol{\alpha}^I \quad (\text{A5})$$

APPENDIX B

Element Manual : Bilinear Degenerated Shell (BDS) Element

ELEMENT DESCRIPTION

- a) Geometry : 4-node bilinear quadrilateral mid-surface, uniform or non-uniform thickness.
- b) Material : linear elastic.
- c) Applications : infinitesimal displacement analysis of
 - shells (thick, thin, non-uniform),
 - membranes,
 - deep beams, shear panels,
 - and any thin structures with user's assigned selective integration scheme.

CODING ASPECT

- a) Main program : FEAP74 (by Prof. R.L. Taylor, University of California ,Berkeley).
- b) Element identification : ELM04
- c) Modular subroutines : BMATRIX, CROSSP, JACOBI, LOAD, LOCALX, TRIMUL, TORSION and SPACKD.
- d) Input data cards :

FLOAD, WTABL
(2F10.0) omitted if LCODE = 0

E , ν ,H,LCODE, κ ,ZB, ρ ,IBS
(7F10.0,15)

MA, 'ELM04' Alphanumerical information
(Standard card in MATERIAL section of FEAP)

Notation :

E - Modulus of Elasticity

ν - Posson ratio

H - Uniform thickness (For non-uniform thickness, leave H blank and input nodal thicknesses in VECT(NUMNP,1) array - see section 6 of FEAP Manual)

- LCODE- 1 Dead load
- 2 Uniform load
- 3 Normal pressure
- 4 Water pressure

κ_t - coefficient of torsional stiffness (> 0.1 recommended)

ZB - ZB.ne.0 : all out-of-plane stiffness deleted.

ρ - Material density.

IBS - Selective integration scheme; three digits corresponding to numbers of quadrature points for (bending,inplane shear,transverse shear) see Note. IBS = 441 for shell (default) and IBS = 421 for deep beam.

FLOAD- Load intensity according to

LCODE	Meaning of FLOAD	Direction
1	Specific weight	Global x_3
2	Uniform load/projected area	Global x_3
3	Normal pressure	Local z_3
4	Water pressure	Local z_3

WTABL- x_3 -coordinate of water table for LCODE=4 only

Note

For the case of a deep beam application, the order of element nodal connection must be such that sides 1-4 and 2-3 represent the beam thicknesses at both ends of the beam element. In this case, H becomes the width of the beam. Integration scheme IBS = 421 should be employed. It denotes a two-by-two quadrature being used in evaluating the stiffness due to bending effect (λ -energy), a one-by-two quadrature (the two on the line joining midsides 1-2 and 3-4) the stiffness due to inplane shear effect (μ -energy), and a one-by-one the stiffness due to transverse shear effect.

C C C ENERGIES SPLIT LOOP - ISP=(1,3)=(VOLUMETRIC,INPLANE SHEAR INVARI.)
ISP= 2 =TRANSVERSE SHEAR ENERGY

ISPLT=3
IF(LX(3).EQ.LX(1)) ISPLT=2
DO 399 ISP=1, ISPLT
IBS=ISP
IF(1SP.EQ.3) IBS=1
LL=LX(1SP)
LR=1
IF(LL.EQ.4) LR=2
LS=2
IF(LL.EQ.1) LS=1
GR=(LR/2)/50
GS=(LS/2)/50
WT=(3.0-LR)*(3.0-LS)
CALL SPACKD(D(1,MA),CT,ISP,ISPLT)

C C C GAUSS POINTS LOOP
DO 312 L=1,LL
RR=RG(L)*GR
SS=GG(L)*GS
CALL LOCALX(RR,SS,TT,NDM,OHM)
CALL JACOBI(RR,SS,NDM,OHM)
DO 304 I=1,NEL
CALL BMATRIX(RR,SS,TT,NDM,OHM,I,IBS)
SJAC=SORTR(JAC(1,3))*2+RJAC(2,3))*2+RJAC(3,3))*2)*JAC
DO 302 I=1,3
DO 302 J=1,3
RJAC(I,J)=CT(I,J)*WJ
RJAC(J,I)=RJAC(I,J)
IS=4-IBS
IF(1SP.EQ.3.AND.1SP.EQ.1.AND.D(4,MA).NE.0.0)
ICALL LOAD(NDM,PDF,D(4,MA),D(5,MA),D(6,MA),S,JAC,TT,OHM,P(1,1))
J1=0
DO 364 IJ=1,NEL
K1=0
DO 362 IK=1,IJ
CALL TRIMUL(BU(1,1,IJ),RJAC,BU(1,1,IK),S(J1+1,K1+1),1.0,15,NST)
IF(BZERO.NE.0.0)
ICALL TRIMUL(BR(1,1,IJ),RJAC,BR(1,1,IK),S(J1+4,K1+4),3.0,15,NST)
IF(1BS.EQ.1) GO TO 362
CALL TRIMUL(CR(1,1,IJ),RJAC,CR(1,1,IK),S(J1+4,K1+4),1.0,2,NST)
CALL TRIMUL(BU(1,1,IJ),RJAC,CR(1,1,IK),S(J1+1,K1+4),1.0,2,NST)
CALL TRIMUL(CR(1,1,IJ),RJAC,BU(1,1,IK),S(J1+4,K1+1),1.0,2,NST)
K1=K1+NDF
J1=J1+NDF
CONTINUE
IF(BZERO.EQ.0.0) GO TO 398
IF(1SP.NE.2) GO TO 399

C C C TORSIONAL ENERGY BY 1-POINT QUADRATURE IF D(7) .GT.0
IF(D(7,MA).NE.0.) CALL TORSION(D(1,MA),S,SJAC,TT,OHM,NST,NEL,PDF)
CONTINUE
DO 382 J=1,NST
DO 382 K=1,J
382 S(K,J)=S(J,K)
IF(1SW.EQ.6) GO TO 6361
ISUB=.FALSE.
389 IF(C6.EQ.0.0) RETURN

ELM 62C
ELM 63C
ELM 64C
ELM 65C
ELM 66C
ELM 67C
ELM 68C
ELM 69C
ELM 70C
ELM 71C
ELM 72C
ELM 73C
ELM 74C
ELM 75C
ELM 76C
ELM 77C
ELM 78C
ELM 79C
ELM 80C
ELM 81C
ELM 82C
ELM 83C
ELM 84C
ELM 85C
ELM 86C
ELM 87C
ELM 88C
ELM 89C
ELM 90C
ELM 91C
ELM 92C
ELM 93C
ELM 94C
ELM 95C
ELM 96C
ELM 97C
ELM 98C
ELM 99C
ELM 100C
ELM 101C
ELM 102C
ELM 103C
ELM 104C
ELM 105C
ELM 106C
ELM 107C
ELM 109C
ELM 110C
ELM 111C
ELM 112C
ELM 113C
ELM 114C
ELM 115C

GO TO 5
3531 DO 390 I=1,NST
390 S(I,I)=S(I,I)+C6*P(1,2)
RETURN
C C C
4 NHF=NDF/2
DO 450 J=1,5
EPS(J)=0.0
450 CHI(J)=0.0

C C C COMPUTE STRAIN AND CURVATURE AT CENTER
RR=0.0
SS=0.0
CALL LOCALX(RR,SS,TT,NDM,OHM)
CALL JACOBI(RR,SS,NDM,OHM)
TEMP=2.0/TT
DO 470 I=1,NEL
CALL BMATRIX(RR,SS,TT,NDM,OHM,I,1)
DO 460 K=1,3
TP=UL(K,I)
DO 460 K=1,3
DO 460 J=1,3
EPS(J)=EPS(J)+BU(J,K,I)*TP
460 IF(BZERO.NE.0.) CHI(J)=CHI(J)+BR(J,K,I)*TO
IF(BZERO.EQ.0.0) GO TO 470
CALL BMATRIX(RR,SS,TT,NDM,OHM,I,2)
DO 465 K=1,3
TP=UL(K,I)
DO 465 J=1,2
465 EPS(3+J)=EPS(3+J)+BU(J,K,I)*TP + CR(J,K,I)*TO
470 CONTINUE

C C C COMPUTE STRESS-RESULTANT, COUPLES AT CENTERS
CALL SPACKD(D(1,MA),CT,1,2)
TEMP=TT**3/12.0
DO 475 J=1,3
XO(J,5)=0.0
DO 473 I1=1,NEL
473 XO(J,5)=XO(J,5)+0.25*XO(J,I1)
XN(J)=0.0
XH(J)=0.0
DO 474 K=1,3
XN(J)=XN(J)+CT(J,K)*EPS(K)*TT
XH(J)=XH(J)+CT(J,K)*CHI(K)*TEMP
474 CONTINUE
475 CALL SPACKD(D(1,MA),CT,2,2)
DO 480 K=1,2
XN(3+J)=0.0
DO 480 K=1,2
480 XN(3+J)*XN(3+J)+TT*CT(J,K)*EPS(3+K)
MCT=MCT-I
IF(MCT.GT.0) GO TO 490
URITE(6,2401) 0,HEAD
MCT=50

490 URITE(6,2402) N,MA,(XO(J,5),J=1,3),EPS,(OHM(1,J),J=1,3),
XN,(OHM(2,J),J=1,3),CHI,(OHM(3,J),J=1,3),XM
495 RETURN
C C C 5 DO 512 L=1,4
ELM 116C
ELM 117C
ELM 118C
ELM 119C
ELM 120C
ELM 121C
ELM 122C
ELM 123C
ELM 124C
ELM 125C
ELM 126C
ELM 127C
ELM 128C
ELM 129C
ELM 130C
ELM 131C
ELM 132C
ELM 133C
ELM 134C
ELM 135C
ELM 136C
ELM 137C
ELM 138C
ELM 139C
ELM 140C
ELM 141C
ELM 142C
ELM 143C
ELM 144C
ELM 145C
ELM 146C
ELM 147C
ELM 148C
ELM 149C
ELM 150C
ELM 151C
ELM 152C
ELM 153C
ELM 154C
ELM 155C
ELM 156C
ELM 157C
ELM 158C
ELM 159C
ELM 160C
ELM 161C
ELM 162C
ELM 163C
ELM 164C
ELM 165C
ELM 166C
ELM 167C
ELM 168C
ELM 169C
ELM 170C

```

C ... FORMATS
C
1100 FORMAT(7F10.0,2I5)
2100 FORMAT(5X,7HMODULUS,13X,1H=.G13.4
1 /5X,13HPOISSON RATIO,7X,1H=.G13.4
2 /5X,20HMASS DENSITY
3 /5X,17HCONSTRAINT FACTOR,3X,1H=.G13.4
4 /5X,20HNO OF GAUSS POINT
5 /5X,20HBENDING
6 /5X,20HTRANSVERSE SHEAR
7 /5X,20HTRANSVERSE SHEAR
8 /5X,20HTRANSVERSE SHEAR
9 /5X,20HTRANSVERSE SHEAR
10 /5X,20HTRANSVERSE SHEAR
11 /5X,20HTRANSVERSE SHEAR
12 /5X,20HTRANSVERSE SHEAR
13 /5X,20HTRANSVERSE SHEAR
14 /5X,20HTRANSVERSE SHEAR
15 /5X,20HTRANSVERSE SHEAR
16 /5X,20HTRANSVERSE SHEAR
17 /5X,20HTRANSVERSE SHEAR
18 /5X,20HTRANSVERSE SHEAR
19 /5X,20HTRANSVERSE SHEAR
20 /5X,20HTRANSVERSE SHEAR
21 /5X,20HTRANSVERSE SHEAR
22 /5X,20HTRANSVERSE SHEAR
23 /5X,20HTRANSVERSE SHEAR
24 /5X,20HTRANSVERSE SHEAR
25 /5X,20HTRANSVERSE SHEAR
26 /5X,20HTRANSVERSE SHEAR
27 /5X,20HTRANSVERSE SHEAR
28 /5X,20HTRANSVERSE SHEAR
29 /5X,20HTRANSVERSE SHEAR
30 /5X,20HTRANSVERSE SHEAR
31 /5X,20HTRANSVERSE SHEAR
32 /5X,20HTRANSVERSE SHEAR
33 /5X,20HTRANSVERSE SHEAR
34 /5X,20HTRANSVERSE SHEAR
35 /5X,20HTRANSVERSE SHEAR
36 /5X,20HTRANSVERSE SHEAR
37 /5X,20HTRANSVERSE SHEAR
38 /5X,20HTRANSVERSE SHEAR
39 /5X,20HTRANSVERSE SHEAR
40 /5X,20HTRANSVERSE SHEAR
41 /5X,20HTRANSVERSE SHEAR
42 /5X,20HTRANSVERSE SHEAR
43 /5X,20HTRANSVERSE SHEAR
44 /5X,20HTRANSVERSE SHEAR
45 /5X,20HTRANSVERSE SHEAR
46 /5X,20HTRANSVERSE SHEAR
47 /5X,20HTRANSVERSE SHEAR
48 /5X,20HTRANSVERSE SHEAR
49 /5X,20HTRANSVERSE SHEAR
50 /5X,20HTRANSVERSE SHEAR
51 /5X,20HTRANSVERSE SHEAR
52 /5X,20HTRANSVERSE SHEAR
53 /5X,20HTRANSVERSE SHEAR
54 /5X,20HTRANSVERSE SHEAR
55 /5X,20HTRANSVERSE SHEAR
56 /5X,20HTRANSVERSE SHEAR
57 /5X,20HTRANSVERSE SHEAR
58 /5X,20HTRANSVERSE SHEAR
59 /5X,20HTRANSVERSE SHEAR
60 /5X,20HTRANSVERSE SHEAR
61 /5X,20HTRANSVERSE SHEAR
62 /5X,20HTRANSVERSE SHEAR
63 /5X,20HTRANSVERSE SHEAR
64 /5X,20HTRANSVERSE SHEAR
65 /5X,20HTRANSVERSE SHEAR
66 /5X,20HTRANSVERSE SHEAR
67 /5X,20HTRANSVERSE SHEAR
68 /5X,20HTRANSVERSE SHEAR
69 /5X,20HTRANSVERSE SHEAR
70 /5X,20HTRANSVERSE SHEAR
71 /5X,20HTRANSVERSE SHEAR
72 /5X,20HTRANSVERSE SHEAR
73 /5X,20HTRANSVERSE SHEAR
74 /5X,20HTRANSVERSE SHEAR
75 /5X,20HTRANSVERSE SHEAR
76 /5X,20HTRANSVERSE SHEAR
77 /5X,20HTRANSVERSE SHEAR
78 /5X,20HTRANSVERSE SHEAR
79 /5X,20HTRANSVERSE SHEAR
80 /5X,20HTRANSVERSE SHEAR
81 /5X,20HTRANSVERSE SHEAR
82 /5X,20HTRANSVERSE SHEAR
83 /5X,20HTRANSVERSE SHEAR
84 /5X,20HTRANSVERSE SHEAR
85 /5X,20HTRANSVERSE SHEAR
86 /5X,20HTRANSVERSE SHEAR
87 /5X,20HTRANSVERSE SHEAR
88 /5X,20HTRANSVERSE SHEAR
89 /5X,20HTRANSVERSE SHEAR
90 /5X,20HTRANSVERSE SHEAR
91 /5X,20HTRANSVERSE SHEAR
92 /5X,20HTRANSVERSE SHEAR
93 /5X,20HTRANSVERSE SHEAR
94 /5X,20HTRANSVERSE SHEAR
95 /5X,20HTRANSVERSE SHEAR
96 /5X,20HTRANSVERSE SHEAR
97 /5X,20HTRANSVERSE SHEAR
98 /5X,20HTRANSVERSE SHEAR
99 /5X,20HTRANSVERSE SHEAR
100 /5X,20HTRANSVERSE SHEAR

```

```

ELM171C
ELM172C
ELM173C
ELM174C
ELM175C
ELM176C
ELM177C
ELM178C
ELM179C
ELM180C
ELM181C
ELM182C
ELM183C
ELM184C
ELM185C
ELM186C
ELM187C
ELM188C

ELM189C
ELM190C
ELM191C
ELM192C
ELM193C
ELM194C
ELM195C
ELM196C
ELM197C
ELM198C
ELM199C

ELM200C
ELM201C
ELM202C
ELM203C
ELM204C
ELM205C
ELM206C
ELM207C
ELM208C
ELM209C
ELM210C
ELM211C
ELM212C
ELM213C

ELM214C
ELM215C
ELM216C
ELM217C
ELM218C
ELM219C
ELM220C
ELM221C
ELM222C

C
306 RR=RG(L)/50
307 SS=OG(L)/50
308 CALL LOCALX(ARR,SS,TT,NDM,OHM)
309 CALL JACOBI(ARR,SS,NDM,OHM)
310 SJAC=SQRT(RJAC(1,3)**2+RJAC(2,3)**2+RJAC(3,3)**2)*XJAC
311 XMASS=RO*XJAC*TT
312 RMASS=XMASS*TT/12.0
313 J1=0
314 DO 508 J1=1,NEL
315 DO 306 J1=1,3
316 P(J1+J,2)=P(J1+J,2)+XMASS*SHP(3,I,J)
317 P(J1+J,3,2)=P(J1+J,3,2)+XMASS*SHP(3,I,J)
318 J1=J1+NDP
319 512 CONTINUE
320 IF(1SW.EQ.3)GO TO 3531
321 IF(1SW.EQ.6)GO TO 6561
322 RETURN
323

C
6 IF(D(4,MA).EQ.0.0)GO TO 63
C
C FORM ELEMENT-GENERATED LOAD
C
DO 610 L=1,4
RR=RG(L)/50
SS=OG(L)/50
CALL LOCALX(ARR,SS,TT,NDM,OHM)
CALL JACOBI(ARR,SS,NDM,OHM)
SJAC=SQRT(RJAC(1,3)**2+RJAC(2,3)**2+RJAC(3,3)**2)*XJAC
CALL LOAD(NDM,NDP,D(4,MA),D(5,MA),D(6,MA),SJAC,TT,OHM,F(1,1))
63 DO 630 J1=1,NEI
DO 630 J1=1,NDP
630 IF(UL(C,J,1).NE.0.0)GO TO 3
GO TO 65
C
C FORM INTERNAL FORCE K(U)
C
6361 K1=0
DO 633 K=1,NEL
DO 632 I=1,NDP
TP=UL(I,K)
DO 631 J=1,NST
P(C,J,1)=P(C,J,1)-S(C,J,K,1+1)*TP
632 CONTINUE
633 K1=K1+NDP
ISW5=.TRUE.
65 DO 650 I=1,NEL
DO 650 J=1,NDP
DO 650 K=1,NST
IF(UDDL(J,1).NE.0.0)GO TO 5
RETURN
C
C FORM INERTIAL FORCE M(UDDL)
C
6561 K1=0
DO 653 K=1,NEL
DO 652 I=1,NDP
TP=UDDL(I,K)
DO 651 J=1,NST
P(C,J,1)=P(C,J,1)-P(C,J,2)*TP
652 CONTINUE
653 K1=K1+NDP
RETURN
C

```

```

ELM223C
ELM224C
ELM225C
ELM226C
ELM227C
ELM228C
ELM229C
ELM230C
ELM231C
ELM232C
ELM233C
ELM234C
ELM235C
ELM236C
ELM237C
ELM238C
ELM239C
ELM240C
ELM241C
ELM242C
ELM243C
ELM244C
ELM245C
ELM246C
ELM247C

ELM248C

ELM249C
ELM250C
ELM251C
ELM252C
ELM253C
ELM254C
ELM255C
ELM256C
ELM257C
ELM258C
ELM259C
ELM260C
ELM261C
ELM262C
ELM263C
ELM264C
ELM265C
ELM266C
ELM267C
ELM268C
ELM269C
ELM270C
ELM271C
ELM272C
ELM273C
ELM274C
ELM275C

ELM276C
ELM277C

SUBROUTINE BMATRIX(PR,SS,TT,NDM,OHM,I,1,ISW)
SUBROUTINE TO COMPUTE BND, BNR, WHERE
EM= BND*U+2*BNR*ROTATION
DIMENSION OHM(3,3)
COMMON/SHP/VA(3,3),WV(3,1),X(3),V3(3,4),BNU(3,3,4),BMR(3,3,4),
1 X0(3,5),CR(3,3,4),CT(3,3)
COMMON/ELM04/XJAC,RJAC(3,3),SHP(3,4),BN,B(2,4),R(4),S(4),T(4)
GO TO (1,100),ISW
1 DO 20 J=1,3
DO 20 K=1,3
IF(J.EQ.3) GO TO 10
BNU(J,K,1)=B(J,1)*OHM(K,J)
BMR(J,K,1)=0.0
DO 5 L=1,3
IF(L.EQ.K) GO TO 5
SIGN=1.0
IF(L.GT.K)SIGN=-1.0
LK=6-L-K
BG=V3(LK,1)
BC=V3(LK,2)
BMR(J,K,1)=BMR(J,K,1)+OHM(L,1)*BC*SIGN*(1)/2.0
5 CONTINUE
GO TO 20
10 BNU(3,K,1)=B(2,1)*OHM(K,1)+B(1,1)*OHM(K,2)
BMR(3,K,1)=B(1,1)*BMR(2,K,1)+B(2,1)*BMR(1,K,1)
20 CONTINUE
DO 30 J=1,2
DO 30 K=1,3
BMR(J,K,1)=BMR(J,K,1)+B(J,1)
30 RETURN
C
100 FAC=BND*SHP(3,1)
ES=BSUM*U+2*BNSR*U+CSR*ROTATION
DO 60 J=1,3

```

```

ELM171C
ELM172C
ELM173C
ELM174C
ELM175C
ELM176C
ELM177C
ELM178C
ELM179C
ELM180C
ELM181C
ELM182C
ELM183C
ELM184C
ELM185C
ELM186C
ELM187C
ELM188C

ELM189C
ELM190C
ELM191C
ELM192C
ELM193C
ELM194C
ELM195C
ELM196C
ELM197C
ELM198C
ELM199C

ELM200C
ELM201C
ELM202C
ELM203C
ELM204C
ELM205C
ELM206C
ELM207C
ELM208C
ELM209C
ELM210C
ELM211C
ELM212C
ELM213C

ELM214C
ELM215C
ELM216C
ELM217C
ELM218C
ELM219C
ELM220C
ELM221C
ELM222C

C
306 RR=RG(L)/50
307 SS=OG(L)/50
308 CALL LOCALX(ARR,SS,TT,NDM,OHM)
309 CALL JACOBI(ARR,SS,NDM,OHM)
310 SJAC=SQRT(RJAC(1,3)**2+RJAC(2,3)**2+RJAC(3,3)**2)*XJAC
311 XMASS=RO*XJAC*TT
312 RMASS=XMASS*TT/12.0
313 J1=0
314 DO 508 J1=1,NEL
315 DO 306 J1=1,3
316 P(J1+J,2)=P(J1+J,2)+XMASS*SHP(3,I,J)
317 P(J1+J,3,2)=P(J1+J,3,2)+XMASS*SHP(3,I,J)
318 J1=J1+NDP
319 512 CONTINUE
320 IF(1SW.EQ.3)GO TO 3531
321 IF(1SW.EQ.6)GO TO 6561
322 RETURN
323

C
6 IF(D(4,MA).EQ.0.0)GO TO 63
C
C FORM ELEMENT-GENERATED LOAD
C
DO 610 L=1,4
RR=RG(L)/50
SS=OG(L)/50
CALL LOCALX(ARR,SS,TT,NDM,OHM)
CALL JACOBI(ARR,SS,NDM,OHM)
SJAC=SQRT(RJAC(1,3)**2+RJAC(2,3)**2+RJAC(3,3)**2)*XJAC
CALL LOAD(NDM,NDP,D(4,MA),D(5,MA),D(6,MA),SJAC,TT,OHM,F(1,1))
63 DO 630 J1=1,NEI
DO 630 J1=1,NDP
630 IF(UL(C,J,1).NE.0.0)GO TO 3
GO TO 65
C
C FORM INTERNAL FORCE K(U)
C
6361 K1=0
DO 633 K=1,NEL
DO 632 I=1,NDP
TP=UL(I,K)
DO 631 J=1,NST
P(C,J,1)=P(C,J,1)-S(C,J,K,1+1)*TP
632 CONTINUE
633 K1=K1+NDP
ISW5=.TRUE.
65 DO 650 I=1,NEL
DO 650 J=1,NDP
DO 650 K=1,NST
IF(UDDL(J,1).NE.0.0)GO TO 5
RETURN
C
C FORM INERTIAL FORCE M(UDDL)
C
6561 K1=0
DO 653 K=1,NEL
DO 652 I=1,NDP
TP=UDDL(I,K)
DO 651 J=1,NST
P(C,J,1)=P(C,J,1)-P(C,J,2)*TP
652 CONTINUE
653 K1=K1+NDP
RETURN
C

```

ELM333C
ELM334C
ELM335C
ELM336C

CALL CROSS(AJAC(L,I),AJAC(L,I),RJAC(L,I),RJAC(L,I),1)
DO 50 J=1,NDM
DO 50 K=1,NDM
50 RJAC(J,K)=RJAC(J,K)*XJAC

TO DETERMINE B=L(N) AND BN=B(ZETA)
B(1,I)=OHM(I), (N(I)), X
B(2,I)=OHM(2), (N(I)), X
BN=OHM(3), (ZETA), X

ELM337C
ELM338C
ELM339C
ELM340C
ELM341C
ELM342C
ELM343C
ELM344C
ELM345C
ELM346C
ELM347C
ELM348C
ELM349C
ELM350C

DO 14 J=1,2
DO 14 I=1,4
B(J,I)=0,0
DO 12 K=1,3
VA(K)=0,0
DO 10 L=1,2
10 VA(K)=VA(K)+RJAC(K,L)*SHP(L,I)
12 B(J,I)=B(J,I)+VA(K)*OHM(K,J)
14 CONTINUE
BN=0,0
DO 15 J=1,3
15 BN=BN+OHM(J,3)*RJAC(J,3)
RETURN
END

ELM351C

SUBROUTINE LOAD(NDM,NDF,TYPE,F,SR,UMJ,TT,OHM,P)
SUBROUTINE TO COMPUTE GENERALIZED LOAD CORRESPONDING TO EACH LOAD
CASES
COMMON/SHAP/VA(3,3),V(3),LX(3),V3(3,4),BU(3,3,4),BR(3,3,4),XD(3,5)
1,CR(3,3,4),CT(3,3)
COMMON/ELM04/XJAC,RJAC(3,3),SHP(3,3),BN,B(2,4),R(4),S(4),T(4)
DIMENSION OHM(3,3),P(1)
NJ=1
JJ=0
IF(TYPE,GE,3,0)NJ=3
H=1,0
IF(TYPE,LE,3,0)GO TO 20
H=0,0
DO 25 I=1,4
DO 25 J=1,4
25 H=H+SHP(3,I)*XD(3,I)
IF(CX-R-H)
DO 32 I=1,4
DO 30 K=1,NJ
J=4-K
A=OHM(J,3)*H
IF(TYPE,EO,2,0)A=OHM(3,3)
IF(TYPE,EO,1,0)A=-TT
30 P(JJ+J)=P(JJ+J)+SHP(3,I)*A*UMJ
32 JJ=JJ+NDF
RETURN
END

C C

ELM376C
ELM377C
ELM378C
ELM379C
ELM380C
ELM381C

SUBROUTINE LOCALX(BR,SS,TT,NDM,OHM)
COMMON/SHAP/VA(3,3),V(3),LX(3),V3(3,4),BU(3,3,4),BR(3,3,4),XD(3,5)
1,CR(3,3,4),CT(3,3)
COMMON/ELM04/XJAC,RJAC(3,3),SHP(3,3),BN,B(2,4),R(4),S(4),T(4)
DIMENSION OHM(3,3)
TT=0,0

ELM278C
ELM279C
ELM280C
ELM281C
ELM282C
ELM283C
ELM284C
ELM285C
ELM286C
ELM287C
ELM288C
ELM289C
ELM290C
ELM291C
ELM292C
ELM293C
ELM294C
ELM295C

DO 60 K=1,3
CR(J,K,I)=0,0
DO 65 L=1,3
IF(L,EO,K)GO TO 65
SIGN=1,0
IF(L,GT,K)SIGN=-1,0
LK=6-L-K
RC=V3(LK,I)
IF(LK,EO,2)BC=-BC
CR(J,K,I)=CR(J,K,I)+OHM(L,I)*RC*SIGN*(I)/2,0
65 CONTINUE
IF(CJ,LT,3)CR(J,K,I)=CR(J,K,I)*FAC
60 BHU(J,K,I)=B(J,I)*OHM(K,3)
DO 70 J=1,2
DO 70 K=1,3
70 BHR(J,K,I)=B(J,I)*CR(3,K,I)
RETURN
END

ELM296C
ELM297C
ELM298C
ELM299C
ELM300C
ELM301C
ELM302C
ELM303C
ELM304C
ELM305C
ELM306C

SUBROUTINE CROSS(A,B,C,IN)
SUBROUTINE TO FINE CROSS-PRODUCT (A*B)=C, AND NORMALIZED IF IN=0
DIMENSION C(3),B(3),A(3)
C(1)=A(2)*B(3)-A(3)*B(2)
C(2)=A(3)*B(1)-A(1)*B(3)
C(3)=A(1)*B(2)-A(2)*B(1)
IF(IN,NE,0)RETURN
CROSS=SDRT(C(1)*C(1)+C(2)*C(2)+C(3)*C(3))
DO 1 I=1,3
1 C(I)=C(I)/CROSS
RETURN
END

ELM307C
ELM308C
ELM309C
ELM310C
ELM311C

SUBROUTINE JACOBI(CR,SS,NDM,OHM)
COMMON/ELM04/XJAC,RJAC(3,3),SHP(3,3),V3(3,4),BN,B(2,4),R(4),S(4),T(4)
COMMON/SHAP/VA(3,3),V(3),LX(3),V3(3,4),BU(3,3,4),BR(3,3,4),XD(3,5)
1,CR(3,3,4),CT(3,3)
DIMENSION OHM(3,3)
FIND JACOBIAN MATRIC, DETERMINANT AND INVERSE-AJAC,XJAC,RJAC
DO 35 K=1,NDM
AJAC(K,3)=0,0
DO 35 J=1,2
AJAC(K,J)=0,0
DO 30 I=1,4
30 AJAC(K,J)=AJAC(K,J)+SHP(J,I)*XD(K,I)
35 CONTINUE
DO 20 I=1,4
TP=SHP(3,I)*T(I)/2,0
DO 25 K=1,3
25 AJAC(K,3)=AJAC(K,3)+V3(K,I)*TP
20 XJAC=0,0
DO 40 J=1,NDM
J2=J+1
J3=J+2
IF(J3,GT,3) J3=J3-3
IF(J2,GT,3) J2=J2-3
40 CALL XJAC+AJAC(I,J)*(AJAC(2,J2)+AJAC(3,J3)-AJAC(2,J3)+AJAC(3,J2))
CALL CROSS(AJAC(1,2),AJAC(1,3),RJAC(1,1),1)
CALL CROSS(AJAC(1,3),AJAC(1,1),RJAC(1,2),1)

ELM312C
ELM313C
ELM314C
ELM315C
ELM316C
ELM317C
ELM318C
ELM319C
ELM320C
ELM321C
ELM322C
ELM323C
ELM324C
ELM325C
ELM326C
ELM327C
ELM328C
ELM329C
ELM330C
ELM331C
ELM332C

DO 40 J=1,4
DO 30 K=1,NDM
AJAC(K,3)=0,0
DO 35 J=1,2
AJAC(K,J)=0,0
DO 30 I=1,4
30 AJAC(K,J)=AJAC(K,J)+SHP(J,I)*XD(K,I)
35 CONTINUE
DO 20 I=1,4
TP=SHP(3,I)*T(I)/2,0
DO 25 K=1,3
25 AJAC(K,3)=AJAC(K,3)+V3(K,I)*TP
20 XJAC=0,0
DO 40 J=1,NDM
J2=J+1
J3=J+2
IF(J3,GT,3) J3=J3-3
IF(J2,GT,3) J2=J2-3
40 CALL XJAC+AJAC(I,J)*(AJAC(2,J2)+AJAC(3,J3)-AJAC(2,J3)+AJAC(3,J2))
CALL CROSS(AJAC(1,2),AJAC(1,3),RJAC(1,1),1)
CALL CROSS(AJAC(1,3),AJAC(1,1),RJAC(1,2),1)

```

ELM362C
ELM363C
ELM364C
ELM365C
ELM366C
ELM367C
ELM368C
ELM369C
ELM370C
ELM371C
ELM372C
ELM373C
ELM374C
ELM375C
ELM376C
ELM377C
ELM378C
ELM379C
ELM380C
ELM381C
ELM382C
ELM383C
ELM384C
ELM385C
ELM386C
ELM387C
ELM388C
ELM389C
ELM390C
ELM391C
ELM392C
ELM393C
ELM394C
ELM395C
ELM396C
ELM397C
ELM398C
ELM399C
ELM400C
ELM401C

```

```

SUBROUTINE TRIMUL(A,B,C,ABC,FAC,IB,NST)
DIMENSION A(3,3),B(3,3),C(3,3),ABC(NST,3),S(3)
DO 200 I=1,NST
DO 250 L=1,3
DO 100 K=1,3
DO 150 J=1,3
TEMP=0.0
TEMP=TEMP+B(J,K)*C(K,L)
S(J)=TEMP
DO 200 I=1,NST
TEMP=0.0
TEMP=TEMP+A(J,I)*S(I)
ABC(I,L)=ABC(I,L)+TEMP/FAC
RETURN
END

```

```

ELM402C
ELM403C
ELM404C
ELM405C
ELM406C
ELM407C
ELM408C
ELM409C
ELM410C
ELM411C
ELM412C
ELM413C
ELM414C
ELM415C
ELM416C
ELM417C
ELM418C
ELM419C
ELM420C
ELM421C
ELM422C
ELM423C
ELM424C
ELM425C
ELM426C
ELM427C
ELM428C
ELM429C
ELM430C

```

```

SUBROUTINE TORSION(D,S,US,TT,OHM,NST,NEL,NDF)
DIMENSION D(1),S(NST,1),OHM(3,3)
COMMON/ELM04/XJAC,RJAC(3,3),SHP(3,4),BN,B(2,4),R(4),O(4),T(4)
I,CR(3,3,4),CT(3,3)
GG=CT(1,1)*1.2
DO 10 J=1,NST
DO 20 I=1,3
DO 30 K=1,3
DO 40 L=1,3
DO 50 M=1,3
DO 60 N=1,3
DO 70 O=1,3
DO 80 P=1,3
DO 90 Q=1,3
DO 100 R=1,3
DO 110 S=1,3
DO 120 T=1,3
DO 130 U=1,3
DO 140 V=1,3
DO 150 W=1,3
DO 160 X=1,3
DO 170 Y=1,3
DO 180 Z=1,3
DO 190 AA=1,3
DO 200 AB=1,3
DO 210 AC=1,3
DO 220 AD=1,3
DO 230 AE=1,3
DO 240 AF=1,3
DO 250 AG=1,3
DO 260 AH=1,3
DO 270 AI=1,3
DO 280 AJ=1,3
DO 290 AK=1,3
DO 300 AL=1,3
DO 310 AM=1,3
DO 320 AN=1,3
DO 330 AO=1,3
DO 340 AP=1,3
DO 350 AQ=1,3
DO 360 AR=1,3
DO 370 AS=1,3
DO 380 AT=1,3
DO 390 AU=1,3
DO 400 AV=1,3
DO 410 AW=1,3
DO 420 AX=1,3
DO 430 AY=1,3
DO 440 AZ=1,3
DO 450 BA=1,3
DO 460 BB=1,3
DO 470 BC=1,3
DO 480 BD=1,3
DO 490 BE=1,3
DO 500 BF=1,3
DO 510 BG=1,3
DO 520 BH=1,3
DO 530 BI=1,3
DO 540 BJ=1,3
DO 550 BK=1,3
DO 560 BL=1,3
DO 570 BM=1,3
DO 580 BN=1,3
DO 590 BO=1,3
DO 600 BP=1,3
DO 610 BQ=1,3
DO 620 BR=1,3
DO 630 BS=1,3
DO 640 BT=1,3
DO 650 BU=1,3
DO 660 BV=1,3
DO 670 BW=1,3
DO 680 BX=1,3
DO 690 BY=1,3
DO 700 BZ=1,3
DO 710 CA=1,3
DO 720 CB=1,3
DO 730 CC=1,3
DO 740 CD=1,3
DO 750 CE=1,3
DO 760 CF=1,3
DO 770 CG=1,3
DO 780 CH=1,3
DO 790 CI=1,3
DO 800 CJ=1,3
DO 810 CK=1,3
DO 820 CL=1,3
DO 830 CM=1,3
DO 840 CN=1,3
DO 850 CO=1,3
DO 860 CP=1,3
DO 870 CQ=1,3
DO 880 CR=1,3
DO 890 CS=1,3
DO 900 CT=1,3
DO 910 CU=1,3
DO 920 CV=1,3
DO 930 CW=1,3
DO 940 CX=1,3
DO 950 CY=1,3
DO 960 CZ=1,3
DO 970 DA=1,3
DO 980 DB=1,3
DO 990 DC=1,3
DO 1000 DD=1,3
DO 1010 DE=1,3
DO 1020 DF=1,3
DO 1030 DG=1,3
DO 1040 DH=1,3
DO 1050 DI=1,3
DO 1060 DJ=1,3
DO 1070 DK=1,3
DO 1080 DL=1,3
DO 1090 DM=1,3
DO 1100 DN=1,3
DO 1110 DO=1,3
DO 1120 DP=1,3
DO 1130 DQ=1,3
DO 1140 DR=1,3
DO 1150 DS=1,3
DO 1160 DT=1,3
DO 1170 DU=1,3
DO 1180 DV=1,3
DO 1190 DW=1,3
DO 1200 DX=1,3
DO 1210 DY=1,3
DO 1220 DZ=1,3
DO 1230 EA=1,3
DO 1240 EB=1,3
DO 1250 EC=1,3
DO 1260 ED=1,3
DO 1270 EE=1,3
DO 1280 EF=1,3
DO 1290 EG=1,3
DO 1300 EH=1,3
DO 1310 EI=1,3
DO 1320 EJ=1,3
DO 1330 EK=1,3
DO 1340 EL=1,3
DO 1350 EM=1,3
DO 1360 EN=1,3
DO 1370 EO=1,3
DO 1380 EP=1,3
DO 1390 EQ=1,3
DO 1400 ER=1,3
DO 1410 ES=1,3
DO 1420 ET=1,3
DO 1430 EU=1,3
DO 1440 EV=1,3
DO 1450 EW=1,3
DO 1460 EX=1,3
DO 1470 EY=1,3
DO 1480 EZ=1,3
DO 1490 FA=1,3
DO 1500 FB=1,3
DO 1510 FC=1,3
DO 1520 FD=1,3
DO 1530 FE=1,3
DO 1540 FF=1,3
DO 1550 FG=1,3
DO 1560 FH=1,3
DO 1570 FI=1,3
DO 1580 FJ=1,3
DO 1590 FK=1,3
DO 1600 FL=1,3
DO 1610 FM=1,3
DO 1620 FN=1,3
DO 1630 FO=1,3
DO 1640 FP=1,3
DO 1650 FQ=1,3
DO 1660 FR=1,3
DO 1670 FS=1,3
DO 1680 FT=1,3
DO 1690 FU=1,3
DO 1700 FV=1,3
DO 1710 FW=1,3
DO 1720 FX=1,3
DO 1730 FY=1,3
DO 1740 FZ=1,3
DO 1750 GA=1,3
DO 1760 GB=1,3
DO 1770 GC=1,3
DO 1780 GD=1,3
DO 1790 GE=1,3
DO 1800 GF=1,3
DO 1810 GG=1,3
DO 1820 GH=1,3
DO 1830 GI=1,3
DO 1840 GJ=1,3
DO 1850 GK=1,3
DO 1860 GL=1,3
DO 1870 GM=1,3
DO 1880 GN=1,3
DO 1890 GO=1,3
DO 1900 GP=1,3
DO 1910 GQ=1,3
DO 1920 GR=1,3
DO 1930 GS=1,3
DO 1940 GT=1,3
DO 1950 GU=1,3
DO 1960 GV=1,3
DO 1970 GW=1,3
DO 1980 GX=1,3
DO 1990 GY=1,3
DO 2000 GZ=1,3
DO 2010 HA=1,3
DO 2020 HB=1,3
DO 2030 HC=1,3
DO 2040 HD=1,3
DO 2050 HE=1,3
DO 2060 HF=1,3
DO 2070 HG=1,3
DO 2080 HH=1,3
DO 2090 HI=1,3
DO 2100 HJ=1,3
DO 2110 HK=1,3
DO 2120 HL=1,3
DO 2130 HM=1,3
DO 2140 HN=1,3
DO 2150 HO=1,3
DO 2160 HP=1,3
DO 2170 HQ=1,3
DO 2180 HR=1,3
DO 2190 HS=1,3
DO 2200 HT=1,3
DO 2210 HU=1,3
DO 2220 HV=1,3
DO 2230 HW=1,3
DO 2240 HX=1,3
DO 2250 HY=1,3
DO 2260 HZ=1,3
DO 2270 IA=1,3
DO 2280 IB=1,3
DO 2290 IC=1,3
DO 2300 ID=1,3
DO 2310 IE=1,3
DO 2320 IF=1,3
DO 2330 IG=1,3
DO 2340 IH=1,3
DO 2350 II=1,3
DO 2360 IJ=1,3
DO 2370 IK=1,3
DO 2380 IL=1,3
DO 2390 IM=1,3
DO 2400 IN=1,3
DO 2410 IO=1,3
DO 2420 IP=1,3
DO 2430 IQ=1,3
DO 2440 IR=1,3
DO 2450 IS=1,3
DO 2460 IT=1,3
DO 2470 IU=1,3
DO 2480 IV=1,3
DO 2490 IW=1,3
DO 2500 IX=1,3
DO 2510 IY=1,3
DO 2520 IZ=1,3
DO 2530 JA=1,3
DO 2540 JB=1,3
DO 2550 JC=1,3
DO 2560 JD=1,3
DO 2570 JE=1,3
DO 2580 JF=1,3
DO 2590 JG=1,3
DO 2600 JH=1,3
DO 2610 JI=1,3
DO 2620 JJ=1,3
DO 2630 JK=1,3
DO 2640 JL=1,3
DO 2650 JM=1,3
DO 2660 JN=1,3
DO 2670 JO=1,3
DO 2680 JP=1,3
DO 2690 JQ=1,3
DO 2700 JR=1,3
DO 2710 JS=1,3
DO 2720 JT=1,3
DO 2730 JU=1,3
DO 2740 JV=1,3
DO 2750 JW=1,3
DO 2760 JX=1,3
DO 2770 JY=1,3
DO 2780 JZ=1,3
DO 2790 KA=1,3
DO 2800 KB=1,3
DO 2810 KC=1,3
DO 2820 KD=1,3
DO 2830 KE=1,3
DO 2840 KF=1,3
DO 2850 KG=1,3
DO 2860 KH=1,3
DO 2870 KI=1,3
DO 2880 KJ=1,3
DO 2890 KK=1,3
DO 2900 KL=1,3
DO 2910 KM=1,3
DO 2920 KN=1,3
DO 2930 KO=1,3
DO 2940 KP=1,3
DO 2950 KQ=1,3
DO 2960 KR=1,3
DO 2970 KS=1,3
DO 2980 KT=1,3
DO 2990 KU=1,3
DO 3000 KV=1,3
DO 3010 KW=1,3
DO 3020 KX=1,3
DO 3030 KY=1,3
DO 3040 KZ=1,3
DO 3050 LA=1,3
DO 3060 LB=1,3
DO 3070 LC=1,3
DO 3080 LD=1,3
DO 3090 LE=1,3
DO 3100 LF=1,3
DO 3110 LG=1,3
DO 3120 LH=1,3
DO 3130 LI=1,3
DO 3140 LJ=1,3
DO 3150 LK=1,3
DO 3160 LL=1,3
DO 3170 LM=1,3
DO 3180 LN=1,3
DO 3190 LO=1,3
DO 3200 LP=1,3
DO 3210 LQ=1,3
DO 3220 LR=1,3
DO 3230 LS=1,3
DO 3240 LT=1,3
DO 3250 LU=1,3
DO 3260 LV=1,3
DO 3270 LW=1,3
DO 3280 LX=1,3
DO 3290 LY=1,3
DO 3300 LZ=1,3
DO 3310 MA=1,3
DO 3320 MB=1,3
DO 3330 MC=1,3
DO 3340 MD=1,3
DO 3350 ME=1,3
DO 3360 MF=1,3
DO 3370 MG=1,3
DO 3380 MH=1,3
DO 3390 MI=1,3
DO 3400 MJ=1,3
DO 3410 MK=1,3
DO 3420 ML=1,3
DO 3430 MM=1,3
DO 3440 MN=1,3
DO 3450 MO=1,3
DO 3460 MP=1,3
DO 3470 MQ=1,3
DO 3480 MR=1,3
DO 3490 MS=1,3
DO 3500 MT=1,3
DO 3510 MU=1,3
DO 3520 MV=1,3
DO 3530 MW=1,3
DO 3540 MX=1,3
DO 3550 MY=1,3
DO 3560 MZ=1,3
DO 3570 NA=1,3
DO 3580 NB=1,3
DO 3590 NC=1,3
DO 3600 ND=1,3
DO 3610 NE=1,3
DO 3620 NF=1,3
DO 3630 NG=1,3
DO 3640 NH=1,3
DO 3650 NI=1,3
DO 3660 NJ=1,3
DO 3670 NK=1,3
DO 3680 NL=1,3
DO 3690 NM=1,3
DO 3700 NN=1,3
DO 3710 NO=1,3
DO 3720 NP=1,3
DO 3730 NQ=1,3
DO 3740 NR=1,3
DO 3750 NS=1,3
DO 3760 NT=1,3
DO 3770 NU=1,3
DO 3780 NV=1,3
DO 3790 NW=1,3
DO 3800 NX=1,3
DO 3810 NY=1,3
DO 3820 NZ=1,3
DO 3830 OA=1,3
DO 3840 OB=1,3
DO 3850 OC=1,3
DO 3860 OD=1,3
DO 3870 OE=1,3
DO 3880 OF=1,3
DO 3890 OG=1,3
DO 3900 OH=1,3
DO 3910 OI=1,3
DO 3920 OJ=1,3
DO 3930 OK=1,3
DO 3940 OL=1,3
DO 3950 OM=1,3
DO 3960 ON=1,3
DO 3970 OO=1,3
DO 3980 OP=1,3
DO 3990 OQ=1,3
DO 4000 OR=1,3
DO 4010 OS=1,3
DO 4020 OT=1,3
DO 4030 OU=1,3
DO 4040 OV=1,3
DO 4050 OW=1,3
DO 4060 OX=1,3
DO 4070 OY=1,3
DO 4080 OZ=1,3
DO 4090 PA=1,3
DO 4100 PB=1,3
DO 4110 PC=1,3
DO 4120 PD=1,3
DO 4130 PE=1,3
DO 4140 PF=1,3
DO 4150 PG=1,3
DO 4160 PH=1,3
DO 4170 PI=1,3
DO 4180 PJ=1,3
DO 4190 PK=1,3
DO 4200 PL=1,3
DO 4210 PM=1,3
DO 4220 PN=1,3
DO 4230 PO=1,3
DO 4240 PP=1,3
DO 4250 PQ=1,3
DO 4260 PR=1,3
DO 4270 PS=1,3
DO 4280 PT=1,3
DO 4290 PU=1,3
DO 4300 PV=1,3
DO 4310 PW=1,3
DO 4320 PX=1,3
DO 4330 PY=1,3
DO 4340 PZ=1,3
DO 4350 QA=1,3
DO 4360 QB=1,3
DO 4370 QC=1,3
DO 4380 QD=1,3
DO 4390 QE=1,3
DO 4400 QF=1,3
DO 4410 QG=1,3
DO 4420 QH=1,3
DO 4430 QI=1,3
DO 4440 QJ=1,3
DO 4450 QK=1,3
DO 4460 QL=1,3
DO 4470 QM=1,3
DO 4480 QN=1,3
DO 4490 QO=1,3
DO 4500 QP=1,3
DO 4510 QQ=1,3
DO 4520 QR=1,3
DO 4530 QS=1,3
DO 4540 QT=1,3
DO 4550 QU=1,3
DO 4560 QV=1,3
DO 4570 QW=1,3
DO 4580 QX=1,3
DO 4590 QY=1,3
DO 4600 QZ=1,3
DO 4610 RA=1,3
DO 4620 RB=1,3
DO 4630 RC=1,3
DO 4640 RD=1,3
DO 4650 RE=1,3
DO 4660 RF=1,3
DO 4670 RG=1,3
DO 4680 RH=1,3
DO 4690 RI=1,3
DO 4700 RJ=1,3
DO 4710 RK=1,3
DO 4720 RL=1,3
DO 4730 RM=1,3
DO 4740 RN=1,3
DO 4750 RO=1,3
DO 4760 RP=1,3
DO 4770 RQ=1,3
DO 4780 RR=1,3
DO 4790 RS=1,3
DO 4800 RT=1,3
DO 4810 RU=1,3
DO 4820 RV=1,3
DO 4830 RW=1,3
DO 4840 RX=1,3
DO 4850 RY=1,3
DO 4860 RZ=1,3
DO 4870 SA=1,3
DO 4880 SB=1,3
DO 4890 SC=1,3
DO 4900 SD=1,3
DO 4910 SE=1,3
DO 4920 SF=1,3
DO 4930 SG=1,3
DO 4940 SH=1,3
DO 4950 SI=1,3
DO 4960 SJ=1,3
DO 4970 SK=1,3
DO 4980 SL=1,3
DO 4990 SM=1,3
DO 5000 SN=1,3
DO 5010 SO=1,3
DO 5020 SP=1,3
DO 5030 SQ=1,3
DO 5040 SR=1,3
DO 5050 SS=1,3
DO 5060 ST=1,3
DO 5070 SU=1,3
DO 5080 SV=1,3
DO 5090 SW=1,3
DO 5100 SX=1,3
DO 5110 SY=1,3
DO 5120 SZ=1,3
DO 5130 TA=1,3
DO 5140 TB=1,3
DO 5150 TC=1,3
DO 5160 TD=1,3
DO 5170 TE=1,3
DO 5180 TF=1,3
DO 5190 TG=1,3
DO 5200 TH=1,3
DO 5210 TI=1,3
DO 5220 TJ=1,3
DO 5230 TK=1,3
DO 5240 TL=1,3
DO 5250 TM=1,3
DO 5260 TN=1,3
DO 5270 TO=1,3
DO 5280 TP=1,3
DO 5290 TQ=1,3
DO 5300 TR=1,3
DO 5310 TS=1,3
DO 5320 TT=1,3
DO 5330 TU=1,3
DO 5340 TV=1,3
DO 5350 TW=1,3
DO 5360 TX=1,3
DO 5370 TY=1,3
DO 5380 TZ=1,3
DO 5390 UA=1,3
DO 5400 UB=1,3
DO 5410 UC=1,3
DO 5420 UD=1,3
DO 5430 UE=1,3
DO 5440 UF=1,3
DO 5450 UG=1,3
DO 5460 UH=1,3
DO 5470 UI=1,3
DO 5480 UJ=1,3
DO 5490 UK=1,3
DO 5500 UL=1,3
DO 5510 UM=1,3
DO 5520 UN=1,3
DO 5530 UO=1,3
DO 5540 UP=1,3
DO 5550 UQ=1,3
DO 5560 UR=1,3
DO 5570 US=1,3
DO 5580 UT=1,3
DO 5590 UU=1,3
DO 5600 UV=1,3
DO 5610 UW=1,3
DO 5620 UX=1,3
DO 5630 UY=1,3
DO 5640 UZ=1,3
DO 5650 VA=1,3
DO 5660 VB=1,3
DO 5670 VC=1,3
DO 5680 VD=1,3
DO 5690 VE=1,3
DO 5700 VF=1,3
DO 5710 VG=1,3
DO 5720 VH=1,3
DO 5730 VI=1,3
DO 5740 VJ=1,3
DO 5750 VK=1,3
DO 5760 VL=1,3
DO 5770 VM=1,3
DO 5780 VN=1,3
DO 5790 VO=1,3
DO 5800 VP=1,3
DO 5810 VQ=1,3
DO 5820 VR=1,3
DO 5830 VS=1,3
DO 5840 VT=1,3
DO 5850 VU=1,3
DO 5860 VV=1,3
DO 5870 VW=1,3
DO 5880 VX=1,3
DO 5890 VY=1,3
DO 5900 VZ=1,3
DO 5910 WA=1,3
DO 5920 WB=1,3
DO 5930 WC=1,3
DO 5940 WD=1,3
DO 5950 WE=1,3
DO 5960 WF=1,3
DO 5970 WG=1,3
DO 5980 WH=1,3
DO 5990 WI=1,3
DO 6000 WJ=1,3
DO 6010 WK=1,3
DO 6020 WL=1,3
DO 6030 WM=1,3
DO 6040 WN=1,3
DO 6050 WO=1,3
DO 6060 WP=1,3
DO 6070 WQ=1,3
DO 6080 WR=1,3
DO 6090 WS=1,3
DO 6100 WT=1,3
DO 6110 WU=1,3
DO 6120 WV=1,3
DO 6130 WW=1,3
DO 6140 WX=1,3
DO 6150 WY=1,3
DO 6160 WZ=1,3
DO 6170 XA=1,3
DO 6180 XB=1,3
DO 6190 XC=1,3
DO 6200 XD=1,3
DO 6210 XE=1,3
DO 6220 XF=1,3
DO 6230 XG=1,3
DO 6240 XH=1,3
DO 6250 XI=1,3
DO 6260 XJ=1,3
DO 6270 XK=1,3
DO 6280 XL=1,3
DO 6290 XM=1,3
DO 6300 XN=1,3
DO 6310 XO=1,3
DO 6320 XP=1,3
DO 6330 XQ=1,3
DO 6340 XR=1,3
DO 6350 XS=1,3
DO 6360 XT=1,3
DO 6370 XU=1,3
DO 6380 XV=1,3
DO 6390 XW=1,3
DO 6400 XX=1,3
DO 6410 XY=1,3
DO 6420 XZ=1,3
DO 6430 YA=1,3
DO 6440 YB=1,3
DO 6450 YC=1,3
DO 6460 YD=1,3
DO 6470 YE=1,3
DO 6480 YF=1,3
DO 6490 YG=1,3
DO 6500 YH=1,3
DO 6510 YI=1,3
DO 6520 YJ=1,3
DO 6530 YK=1,3
DO 6540 YL=1,3
DO 6550 YM=1,3
DO 6560 YN=1,3
DO 6570 YO=1,3
DO 6580 YP=1,3
DO 6590 YQ=1,3
DO 6600 YR=1,3
DO 6610 YS=1,3
DO 6620 YT=1,3
DO 6630 YU=1,3
DO 6640 YV=1,3
DO 6650 YW=1,3
DO 6660 YX=1,3
DO 6670 YY=1,3
DO 6680 YZ=1,3
DO 6690 ZA=1,3
DO 6700 ZB=1,3
DO 6710 ZC=1,3
DO 6720 ZD=1,3
DO 6730 ZE=1,3
DO 6740 ZF=1,3
DO 6750 ZG=1,3
DO 6760 ZH=1,3
DO 6770 ZI=1,3
DO 6780 ZJ=1,3
DO 6790 ZK=1,3
DO 6800 ZL=1,3
DO 6810 ZM=1,3
DO 6820 ZN=1,3
DO 6830 ZO=1,3
DO 6840 ZP=1,3
DO 6850 ZQ=1,3
DO 6860 ZR=1,3
DO 6870 ZS=1,3
DO 6880 ZT=1,3
DO 6890 ZU=1,3
DO 6900 ZV=1,3
DO 6910 ZW=1,3
DO 6920 ZX=1,3
DO 6930 ZY=1,3
DO 6940 ZZ=1,3

```

```

ELM432C
ELM433C
ELM434C
ELM435C
ELM436C

```

```

SUBROUTINE SPACKD(D,CT,K,L)
DIMENSION D(1),CT(3,3)
SLAM=D(1)*D(2)/(1.0-D(2)*D(2))
THU=D(1)/(1.0+D(2))
DO 5 I=1,3
DO 5 J=1,3
CT(I,J)=0.0
IF(K.EQ.2)GO TO 10
IF(L.EQ.2)GO TO 20
GO TO (30,10,40),K
CT(1,1)=2.0*SLAM*THU/(SLAM+2.0*THU)
CT(1,2)=CT(1,1)
CT(2,1)=CT(1,1)
CT(2,2)=CT(1,1)
RETURN
END

```